UNIVERSITY OF BIRMINGHAM

An experimental investigation of the aerodynamic flows created by lorries travelling in a long platoon

Robertson, Francis; Bourriez, Frederick; He, Mingzhe; Soper, David; Baker, Christopher; Hemida, Hassan; Sterling, Mark

Link to publication on Research at Birmingham portal

An experimental investigation of the aerodynamic flows created by lorries travelling in a long platoon

Francis H. Robertson, Frederick Bourriez,
Mingzhe He, David Soper, Chris Baker
Hassan Hemida, Mark Sterling
School of Engineering, University of Birmingham,
Edgbaston, Birmingham B15 2TT

Abstract

The concept of autonomous road vehicles has recently gained a great deal of technical respectability. Expected advantages over normal driver-controlled vehicles are through increased safety, reliability and fuel efficiency. This paper presents a novel experimental study enabling for the first time a full understanding of the aerodynamic flow development of a long vehicle platoon. Moving model experiments were carried out at the University of Birmingham Transient Aerodynamic Investigation (TRAIN) rig facility on a 1/20th scale eight lorry platoon with three constant vehicle spacings. Slipstream velocity and pressures, as well as simultaneous on-board vehicle surface pressure measurements were made. Results indicated a highly turbulent boundary layer development, with slipstream pulse peaks near the front of each lorry; similar to previous findings on flows around container freight trains. The drag coefficient of an isolated lorry was in agreement with previous studies. There are substantial reductions in aerodynamic drag for the non-leading platoon vehicles. Drag results plateaued towards a constant value within the platoon. Vehicle spacing affected drag values, with decreases of 57% observed for the closest spacing of half a vehicle length, demonstrating the aerodynamic benefits of platooning.

Keywords: Vehicle aerodynamics; lorry; platoon; slipstream; drag reduction; experimental study; model-scale.

1 Introduction

In recent years the concept of driverless or autonomous road vehicles (AVs) has gained a great deal of technical respectability. Much progress has been made on a range of technologies relevant to this concept, including digital mapping, position recognition by lidar and radar systems and advanced vehicle-to-vehicle communications [1]. There are a number of advantages for such vehicles over normal driver-controlled vehicles in terms of safety,

reliability, access for the disabled and increasing the efficiency of road use [2]. The last of which comes about primarily because the vehicles are able to drive close together in platoon formation.

For these reasons, a number of projects have trialled platooning technology. SARTRE (Safe Road Trains for the Environment) is a project by seven companies from four EU countries which aimed to develop a system that enabled platoons to operate on public motorways without any road infrastructure changes [3-5]. The lead vehicle is operated by a driver and the following vehicles are driven automatically by the system, following instructions from the lead vehicle [3]. This system has been successfully tested, with a five-vehicle platoon (2 leading trucks and 3 following cars), on test tracks and public motorways [3-5]. Safety analyses were also conducted to consider the effects of potential system faults, driver error and malicious third-party actions. Another large-scale EU project, COMPANION (Cooperative dynamic formation of platoons for safe and energy-optimized goods transportation), developed on- and off-board user interfaces and systems for the coordination of platoons of heavy-duty vehicles and validated the systems via simulations and trials on public roads [6]. The UK's first heavy goods vehicle platooning trial, commissioned to show how AVs can improve safety and reduce emissions, is also underway [7]. TRL (Transport Research Laboratory) are overseeing the trials on both test tracks and major public roads for platoons of up to three partially self-driving vehicles, where drivers steer all the lorries but acceleration and braking are controlled wirelessly by the lead driver [8]. Platooning has also been explored in other countries, including Germany, Japan and the USA [8]. With projects such as these either completed or underway, it is clear that the use of AVs will soon be widespread. Indeed, it has been estimated that AVs will become commercially available by 2025 [9], with potential economic benefits reaching $200 billion to $1.9 trillion per year [10].

The concept of running vehicles in close formation or a platoon is not an entirely new phenomena wholly associated with AVs. Indeed, it is commonplace to see lorries travelling in tandem on motorways and the concept of using the draft/slipstream for overtaking (one vehicle following closely behind another and travelling in its slipstream to achieve aerodynamic benefits) is commonplace in sports car racing [11] and cycling [12]. When this occurs, there is an increase the pressure at the rear of the leading vehicle due to flow stagnation on the vehicle behind and a reduction in the momentum of the flow approaching the vehicle behind [5,11]. This tends to reduce the drag on both vehicles, which may improve fuel efficiency with benefits such as cost reductions and reduced carbon dioxide emissions. To this end, a number of studies have looked at fuel or power consumption in full-scale vehicle platoons [3-5,13-14]. Indeed, SATRE showed that greater drag reductions and fuel savings can be achieved with smaller inter-vehicle spacing and estimated that by platooning, trucks could save up to 2.8 tons of CO_2 equivalent per year and cars up to 0.1 tons [3,5]. Furthermore, track tests by Veldhuizen et al. [14] showed that there were significant fuel savings (up to 11.7 ± 0.9%) for the trailing vehicle in a platoon of two heavy duty vehicles. However, for this short platoon formation, there were no significant gains as the vehicle spacing was reduced from the current European legal limit of 50 m down to 10 m. For the leading vehicle there were significant gains at close spacing, but the fuel savings were small in comparison to those of the trailing vehicle.

To date only a restricted amount of experimental work has been carried out on the aerodynamics of vehicles travelling in platoons and as such the nature of the flow field

development around a platoon is not well understood. The PATH project [15] investigated various aspects of the aerodynamic effects due to platooning using wind tunnel tests on 1/8th Lumina APV models. The number of vehicles in the platoon varied from 2 up to 4, while the inter-vehicle spacings tested were from 0 up to 3 times vehicle length. The results suggested that significant drag reduction could be achieved, especially in the strong interaction regime case where the inter-vehicle spacing is less than one vehicle length, and more complicated drag behaviour was identified for the cases with inter-vehicle spacing less than half vehicle length. The drag benefits of platoons with different vehicle shapes were also confirmed by other wind tunnel studies [16-18], although the research focused on different aspects such as heterogeneity, and in-line oscillation. Benefits were observed for 1997 Buick LeSabre scale car models, rectangular box models with sharp corners and edges (designed to simulate mini-vans or a buses) [16] and Ahmed bodies [17-18].

It should be noted however, that studies have shown that platooning does not always lead to drag reduction. Experimental results for a platoon of two Ahmed-bodies with a slant angle back [17-18] indicated a drag penalty for the trailing vehicle at small inter-vehicle spacing, opposite to the findings of Zabat et al. [15] for a square back two-vehicle platoon. For backlight angles and vehicle spacings between 25° to 35° and 0.125 to 3 vehicle lengths respectively, no combination yielded drag reductions for both models [17]. Overall benefits were observed for spacings less than half the vehicle length, but this included a significant increase in drag for the trailing vehicle (6-42%). For 30° backlight angles, significant drag increases were found for the rear vehicles for spacings between 0.1 and 1.0 vehicle lengths whilst reductions were observed from 1.0 up to the maximum spacing of 4.0 vehicle lengths [18]. Le Good et al. [19] also reported overall drag penalties for platoons of 3 and 5 cars, with a more streamlined shape than Zabat et al. [15], at a spacing of one-quarter of the vehicle length. However, there was an overall drag benefit when a second parallel line of vehicles was added at a lateral spacing of half the vehicle length and/or when the yaw angle was increased to 15°. Le Good et al. [19] noted that manufacturers tend to test and optimise vehicles to meet emission regulations based on a vehicle driving in isolation, but that a low-drag style of vehicle may not be optimum for an overall drag reduction within a platoon. Indeed, minimising the flow disturbance and the size of the wake of an upwind vehicle, are not conducive to minimising drag on the downwind vehicles. In a further study by Le Good et al. [20], the authors suggest that active aerodynamic features could be tuned to give the maximum overall benefit depending on the platoon configuration and position of vehicles. Results demonstrated that modifications to some of the low-drag style of cars, such as nose and/or backlight add-ons, could result in an overall drag benefit in platoons of 2 to 5 cars at one-quarter length spacing, whereas without the modifications there were consistently penalties. It is worth noting however, that these studies [19-20] were conducted at very low Reynolds number ($7x10^4$ based on the vehicle length).

With the growing ability of Computational Fluid Dynamics (CFD) to accurately and affordably simulate the airflow around vehicles, there has been extensive research that focuses on detailed information of flow around various types of ground vehicles using numerous CFD techniques. Davila et al. [5] conducted Steady-state k-omega Shear Stress Transport (SST) simulations with low Reynolds number near wall treatment for a five-vehicle platoon of mixed shapes, under the same conditions as the SATRE track tests. The CFD confirmed that larger drag reductions can be achieved with smaller inter-vehicle spacing. Vegendla et al. [21] also

performed Reynolds-averaged Navier-Stokes (RANS) simulations on two or three trucks with single and multi-lane scenarios. Yaw-averaged aerodynamic drag was used to estimate a more realistic 'real world' drag coefficient. Drag reductions were predicted for both large and small vehicle distances for two trucks running collinearly. Humphreys and Bevly [22] conducted RANS and Detached Eddy Simulation (DES) on a two-truck platoon using a simplified truck model. The non-physical wake prediction from RANS was identified, compared to the DES results, but the general trend of drag reduction from RANS is regarded as very similar to the DES results if the inter-vehicle spacing is less than 4 vehicle lengths. The CFD derived drag were converted to fuel consumption, with a trend akin to that from field tests. An interesting observation was mentioned that the trailing vehicle experienced certain buffeting, seemingly due to front vehicle wake vortex shedding. Mirzaei and Krajnovic' [23] conducted Large Eddy Simulation (LES) on a two Ahmed body platoon, considering three different vehicle-to-vehicle spacing, namely 0.3, 0.5 and 1 vehicle length, with the aim of exploring the drag penalty phenomena noted by Pagliarella et al. [17] and Watkins and Vino [18]. The LES results show drag penalty at the two smaller inter-vehicle distances which is consistent with that observed in the wind tunnel tests. Jacuzzi and Granlund [24] employed the steady-state SST k-omega turbulence model to investigate the influence of a passively blown duct from the vehicle nose out of the front wheel opening, on the drag on a trailing car in a platoon of two NASCAR Xfinity Series race vehicles. The results, which were validated by full-scale wind tunnel tests, showed that suitably positioned ducts could reduce the drag for all spacings considered.

RANS modelling, validated by wind tunnel tests, has also been used to investigate the aerodynamic drag on a cyclist riding in proximity with other cyclists [12] and with a trailing motorcyclist [25] and car [26]. Blocken et al. [12] conducted simulations, with the Transition k-omega SST model, on a peloton (a group of cyclists riding in proximity to reduce drag and hence energy expenditure) consisting of 121 cyclists. Every cyclist experienced a drag reduction compared to an isolated cyclist. The largest reduction of 95% was obtained by the riders towards the rear of the peloton and towards the middle laterally. Results from simulations with the steady-state standard k-epsilon model showed drag reductions between 8.7% and 3.8% for a cyclist which was followed by a motorcyclist at a separation between 0.25 m and 1 m respectively [25] and between 3.7% and 0.2% when followed by a car at a separation between 3 m and 10 m [26].

Although the wind tunnel and CFD tests on static models generate a great deal of insight on the aerodynamics of platooning, these approaches allows an unrealistic turbulent boundary layer to grow as the flow propagates. A ground suction mechanism was employed by Zabat et al. [15] and Tsuei and Savaş [16] to control the thickness of such an unwanted boundary layer, while it seems that no remedy was taken by Pagliarella et al. [17], Watkins and Vino [18] or Le Good et al. [19-20]. The previous research is also limited as studies have typically concentrated on aerodynamic effects on the platoon itself rather than on the surrounding environment. It is important to also consider the flow development at the vehicle sides as this may affect passing traffic, as well as pedestrians and equipment at the roadside. In addition, there are uncertainties which arise from running vehicles in very close formation related to the overall stability of vehicles travelling in the wake of other vehicles, particularly if there are organised coherent wake flow structures such as trailing vortices. For example, in stock car racing (e.g. NASCAR) there are significant aerodynamic effects on vehicle handling when drafting [11].

Clearly, this is an important safety issue, yet this has received very little attention in the current literature. Similarly, the effects of platooning on driver comfort, e.g. due to buffeting as observed by Humphreys and Belvy [22], have not been investigated extensively. Finally, very limited research [5,19-20] has ever addressed a platoon longer than four vehicles.

This paper describes a series of novel moving model scale experiments, with a platoon of eight box-type lorries, which were undertaken at the University of Birmingham Transient Aerodynamic Investigation (TRAIN) rig facility. The method employed address several limitations of previous research. Firstly, the use of a moving rig correctly simulates the movement of vehicles with respect to the ground, thus realistically modelling the boundary layer development. Secondly, the longer platoon than considered previously, allows investigation of whether any potential drag benefits plateau towards the rear of a platoon of a length appropriate for the practical application of AVs. Finally, the lorries are an accurate model of a vehicle of practical importance as the haulage industry is likely to be an early adopter of AV technology. Conflicting reports on the overall drag reductions (or penalties) clearly demonstrate that any benefit is highly sensitive to the vehicle shape and platoon configuration. Thus, typical commercial box-type lorries are an important test case which is unlikely to be well represented by oversimplified vehicle geometries such as the Ahmed-body.

The experimental work is supplemented by CFD simulations using conventional RANS techniques for a wide range of platoon configurations and a smaller number of calculations using more sophisticated DES methods to provide high quality unsteady flow information. These results provide valuable insight into the aerodynamic behaviour of close-running lorries in a long platoon.

The work presented in this paper focuses on the mean flow from the physical model testing. The first aim is to understand the flow development at vehicle sides and its effect on other road users. The second aim is to understand the mean surface pressure distribution on the vehicles and to estimate the aerodynamic drag to assess the potential benefit of running lorries in a long platoon. These results will provide a benchmark for the validation of CFD predictions and the calibration of models, which is to be presented elsewhere. Ultimately, this will improve accuracy in predictions of the drag coefficient as here this is estimated from the pressure measurements at a limited number of locations. The project will also investigate the lateral stability of vehicles travelling in the wake of other vehicles by analysing both the experimental and CFD data. However, for the sake of brevity, unsteady flow will be considered in a separate experimental paper.

The TRAIN rig facility and moving models are described in detail in sections 2.1-2.2. The experiment instrumentation for both sets of measurements are introduced in section 2.3, and the analysis methods in section 2.4. Results are initially presented for the aerodynamic flow development at the vehicle side in section 3.1 where comparisons are drawn to other vehicle types and the significance of this for passing traffic is discussed. This is developed to look at the on-board surface pressure results and analyse effects due to the vehicles travelling in a platoon with different spacings between the vehicles in section 3.2 and mean drag coefficients are presented in section 3.3. Finally, the main conclusions are presented in section 4.

2 Experiment methodology

2.1 TRAIN rig facility

Correctly modelling the relative movement between a vehicle with respect to the ground is often cited a difficult task in experimental aerodynamic studies [15-16] due to limitations in wind tunnel capabilities. The use of moving-model experiment facilities to measure vehicle aerodynamics has increased dramatically over the last 20 years due to the capability of correctly simulating the movement of a vehicle in respect to a fixed ground plane. The University of Birmingham Transient Aerodynamic Investigation (TRAIN) rig is a moving-model facility, purpose-built to examine the transient aerodynamics of moving vehicles [27]. Model vehicles of various scales are propelled along a series of 150 m long tracks at speeds up to 75 m/s, dependent on model weight. This methodology works well when simulating a single vehicle or a train composed of a number of carriages jointed together. The firing mechanism, discussed at length by Soper et al. [28], however prevents multiple individual models being fired in quick succession to create a platoon type effect. To overcome this limitation, a novel approach was applied in this study by which a set of model vehicles in a platoon configuration were mounted to a long spine type system and run through a slot gap set between a suspended ground plane to simulate the normal ground condition. The suspended ground plane and platoon of lorries are shown in Figure 1.

Figure 1: The suspended ground plane and platoon of lorries.

The suspended ground plane was 20 m in length and set up at a suitable position along the facility test section to ensure that the model vehicles were travelling at a stable maximum speed. The two ground plane halves were 220 mm and 165 mm in width and set at a distance of 20 mm apart centrally about the centre line of the platoon vehicles. Preliminary tests with

probes placed close to the ground plane edge recorded flow speeds below the lower limit of the measuring instrumentation and as such the ground plane width was not considered to effect the flow development in the areas of interest. The slot gap was minimised to 5 mm each side about the vehicle mounting posts to reduce any effects on the aerodynamic flow around the vehicles due to the mounting system moving through the gap. Further information regarding the general set up of the TRAIN rig and modelling techniques used can be found in Soper et al. [28].

Multiple runs of the experiment were conducted to enable the calculation of ensemble averages of velocities and pressure coefficients. For the slipstream and surface pressure measurements respectively 20 and 15 runs were conducted. Further details on how the data were analysed are given in section 2.4.

2.2 Platoon models

The platoon consists of eight 1/20th scale model box-type lorries. For comparison, a single lorry in isolation was also considered. The dimensions are shown in figure 2. The room walls are 3.8 m apart giving a blockage ratio of 3.3%. The models were based on Leyland DAF 45-130, which was chosen as the shape is 'typical' of a commercial vehicle [29] and because the aerodynamic flow around a single lorry has been investigated previously [29-32], providing surface pressure data for validation of the scale-modelling [29]. Furthermore, direct drag measurements from model-scale wind tunnel tests [31] and LES results [32] provide data to validate the approach used to estimate drag coefficient (see sections 2.4 and 3.4).

The vehicles were modelled in glass reinforced plastic (GRP) from moulds cut directly from a CAD model, shown in figure 2. A number of simplifications were made to conduct the experiments at model-scale. Detailed components such as wing mirrors and underbody skirts were either geometrically simplified or removed. Simplifications of a similar manner have been previously adopted for model-scale studies where such features have been identified as additional small-scale turbulence inducers [27, 34].
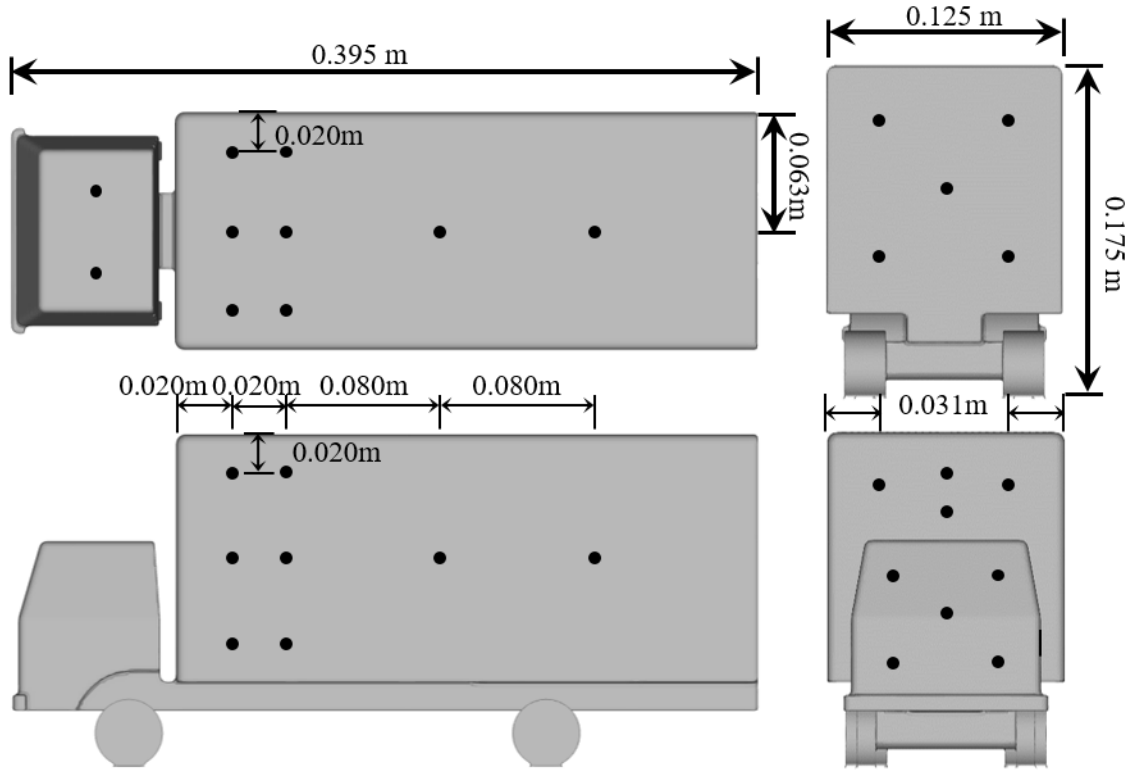
7

Figure 2: Detailed drawing the lorry model including key dimensions and pressure measuring positions.

The chosen number of eight vehicles in the platoon was based on the need to ensure a well-developed boundary layer to allow the interaction between different vehicles in the platoon to be accurately measured. This was estimated based on prior aerodynamic knowledge presented in [33]. The model vehicles were mounted to a long spine system which was in turn fitted with the necessary firing chassis required at the TRAIN rig [28]. The mounting method allowed the vehicles to be freely moved along the spine and thus a number of test positions examined. Nominal vehicle spacings of 0.5L, 1.0L and 1.5L were chosen, where L is the maximum vehicle length of 0.395 m. Throughout this study a platoon speed, V_{plat} = 25 ± 1 m/s (55.9 ± 2.2 mph), was chosen to reflect typical road speeds. This was close to the maximum speed achievable with the TRAIN rig setup (based on the significant vehicle weight) given that the firing mechanism is essentially a tensioned elastic bungee cord. The corresponding Reynolds number is of the order of 3x10^5, based on a lorry height at 1/20th scale. A small model speed decay was observed through the test section, caused by friction and aerodynamic drag. A number of light gate positions enabled an accurate value of model speed at each measuring position to be calculated. A minimum of two connected lorries were required because of the methodology employed through the on-board pressure monitoring systems (see section 2.3). Hence, to represent the 'single' vehicle case a large spacing of 14L between a pair of vehicles was used to ensure that the lead vehicle was effectively isolated.

8

2.3 Measuring instrumentation and coordinate system

A series of measurements were made on and around the platoon to measure surface pressure and aerodynamic properties of the vehicle slipstream. The boundary layer development of slipstream velocities and static pressure were measured by multi-hole pressure probes, manufactured by Turbulent Flow Instrumentation [35]. The probes are capable of measuring local static pressure and three components of velocity instantaneously, within calibrated bounds of 0.5 m/s, 5 Pa and ±1° for velocities, static pressure and flow direction respectively. Velocities with a magnitude lower than 2 m/s have a higher uncertainty associated with the calibration of the probes. A potential drawback of these probes when measuring highly turbulent air flows is a ±45° cone of acceptance. Previous studies on slipstream flows have highlighted that the majority of the flow occurs within flow angles of ±20° [36]. Indeed, average flow angles, calculated from results measured in this study indicate a similar range of values. Measurements were made at a sampling frequency of 5 kHz. All data were filtered using a 650 Hz low-pass filter to reflect the maximum frequency response of the probe [28]. All slipstream data measured at the vehicle side were resampled with respect to the nominal vehicle speed to account for small differences in speed between test runs. Multi-hole probe measurements were made with a series of rakes of probes for a number of lateral and vertical positions from the vehicle side and above the ground plane, as indicated in table 1. The displacement of -1.25 m from the lorry side, at full-scale, is along the lateral centreline of the vehicles. Measurements to the side of the vehicles were taken near the mid-wheel height, mid-vehicle height and just below the top of the vehicle. Slipstream measurements were only conducted for the three platoon configurations, not for the single lorry.

Distance above ground plane (m)	Displacement from the lorry side (m)			
	-1.25	0.25	0.50	1.00
0.4	-	X	X	X
0.6	-	X	X	X
3.0	-	X	X	X
3.75	X	-	-	-
4.25	X	-	-	-
4.75	X	-	-	-

Table 1: Multi-hole probe measuring positions for the lorries. All dimensions are given as the full-scale equivalent. X indicates that a measurement was made at the selected position.

As well as roadside measurements, the pressure development on the surface of the vehicles was also measured. A series of custom-built on-board pressure monitoring systems with stand-alone data loggers were built into all vehicles (taking the first vehicle in the platoon as lorry 1 and the last vehicle as lorry 8 etc). The system in each vehicle consists of a stand-alone data logger powered by a rechargeable battery, connected via a bespoke circuit board system to fourteen miniaturised differential pressure transducers manufactured by FirstSensor Ltd [37].

A light detector was also set up in each vehicle and the outputted data is linked to all the other vehicles to act as a sync and position finder in each data set. The pressure transducer measuring ports were connected via silicon tubing to metal tubing adapters glued into the vehicle walls, acting as pressure taps. The pressure transducer reference ports were connected via silicon tubing to a manifold in each vehicle. The manifolds were in turn connected to each other and attached to a sealed reservoir, acting as a synchronised on-board reference pressure system for the whole platoon. To negate any possible effects of drift in the sealed reservoir, created by variations in ambient temperature, a vent was fitted into the system which was opened after every run. The purpose-built stand-alone data logger has a 16-bit resolution and is capable of monitoring 15 channels at a maximum sampling rate of 3 kHz. A series of pressure tap loops were positioned on the vehicles, as well as nominal points on the lead and rear vehicle faces, as shown in figure 2. It should be noted that no pressure taps were placed on the vehicle underside because the monitoring system was mounted such that it covered the internal base area of the vehicle.

The model speed was measured using a series of opposing photoelectric position finders and reflectors set up along the ground plane. Speed was calculated based on the time taken for the model to break both beams, to an accuracy of ±0.1 m/s. All position finder data were recorded and could be used to assist in aligning data. Measured vehicle speeds were within 4% of the nominal speed of 25 m/s. Ambient conditions were monitored using a weather station to measure room temperature T and relative humidity Φ, with an uncertainty of ±2 °C and ±10% respectively, and a digital barometer to measure atmospheric pressure P_{atm}, with an uncertainty of ±0.2 kPa. Air density ρ was calculated using the gas constant $R = 287$ (J/kg K), and the measured T, Φ and P_{atm}. The mean ± standard deviation of ambient conditions, from the surface pressure measurements, are as follows: $P_{atm} = 101.0 \pm 0.8$ kPa, $T = 18.3 \pm 2.2$ °C, $\Phi = 54 \pm 6$ and $\rho = 1.210 \pm 0.015$ kgm^{-3}.

A coordinate system is adopted such that the x-axis is aligned in the direction of vehicle travel with the origin either taken to be front of the first vehicle or the front of each vehicle examined for the slipstream and on-board pressure measurements respectively. The y-axis is taken as a horizontal plane perpendicular to the direction of vehicle travel and the z-axis is in the vertical direction measured from the ground plane. Mean surface pressure coefficients are presented along lines x_1 and x_s. x_1 is a line around the front pressure loop, which is a slice through the lorry 0.4 m from the front of the box-section relative to full-scale, with the origin at $y = 0$. x_s is a line around a slice through the symmetry plane of the lorries ($y = 0$), with the origin at the centre of the cab front. All distances in figures or captions are expressed relative to full-scale.

2.4 Analysis methodology

A series of analysis methodologies were adopted depending on the measurement type. For the boundary layer slipstream measurements, a series of 20 runs were conducted for each measuring position to enable an ensemble average to be calculated. Raw data from each run was aligned with the nose of lorry 1, indicated by the position finder data, and resampled with respect to the nominal platoon speed to account for small differences in model speed between runs. Properties of the aerodynamic flow are presented as non-dimensional coefficients to aid comparison of results,

$$U(\tau) = \frac{u(\tau)}{V_{plat}} \tag{1}$$

$$V(\tau) = \frac{v(\tau)}{V_{plat}} \tag{2}$$

$$W(\tau) = \frac{w(\tau)}{V_{plat}} \tag{3}$$

$$U_{res}(\tau) = \sqrt{\left(\frac{u(\tau)}{V_{plat}}\right)^2 + \left(\frac{v(\tau)}{V_{plat}}\right)^2} \tag{4}$$

$$I_u(\tau) = \frac{\sigma_u(\tau)}{1-U(\tau)} \tag{5}$$

$$C_P(\tau) = \frac{p(\tau)-p_0}{\frac{1}{2}\rho V_{plat}^2} \tag{6}$$

where (U,V,W) is the normalised velocity vector and (u,v,w) is the velocity in relation to (x,y,z). The dimensionless time, τ is taken as 0 and 1 respectively as the nose and the rear of the first lorry pass the multi-hole probe, i.e. $\tau = V_{plat}t/L$ where t is the time since the lorry has passed. The dimensionless time taken for each lorry to pass the pressure probes is indicated by shaded rectangles on figures 3-8. U_{res} is the overall normalised horizontal velocity. I_u is the longitudinal turbulence intensity and σ_u is the standard deviation of U from individual runs in relation to the ensemble mean,

$$\sigma_u(\tau) = \sqrt{\frac{1}{R}\sum_r (U_r(\tau) - U(\tau))^2} \tag{7}$$

where U_r is the normalised longitudinal component of velocity for a given run, r, and R is the total number of runs (20). To calculate $(U_r - U)^2$ for a given run, U was first resampled with respect to the measured platoon speed. $(U_r - \overline{U})^2$ for each run was then resampled with respect to the nominal speed before finding the ensemble average of this quantity. As the platoon is moving in relation to the measuring equipment, the denominator of $1-U$ in equation 6 ensures that the right frame of reference is considered [35], as opposed to U if the vehicles and equipment were in the same reference frame. The coefficient of pressure C_P in equation 7 is calculated at model-scale with respect to an ambient reference pressure, p_0, and the air density, ρ.

The lorry surface pressure measurements are similarly presented in terms of non-dimensional pressure coefficients, derived from time averaging the coefficient time history. Surface pressure data for each lorry are initially aligned and cropped with respect to the test section via the position finder data. To ensure the lorry velocity is approximately constant, the surface pressure data are truncated to their values when lorry 1 is between the light gates. The maximum difference between the average vehicle speed between all five light gates and the speed through a single 1 m section is 3.2%. The raw voltage data from each

transducer are converted to pressure through a series of equations based on a set of detailed Betz manometer and tube length correction calibrations. Before the platoon is fired the initially recorded data measures the ambient room pressure in relation to the sealed reference pressure. A short (5 s) section of data is averaged and subtracted from the whole pressure trace for each run. This effectively eliminates the reference pressure in the calculation and leaves the pressure in relation to the ambient room pressure. The resulting differential pressure, $p(\tau)-p_0$, is non-dimensionalised, as in equation 6. The time history of the pressure coefficient is then averaged for each run and the mean pressure coefficient is calculated as the ensemble average across a minimum of 15 runs.

The uncertainty in surface pressure coefficients (shown on figures 9-11) is calculated as the sum of the bias limit and random uncertainty. The former accounts for the characteristics and performance limits of the instrumentation and the latter accounts for run to run variability relating to flow unsteadiness [38]. The bias limit for pressure coefficients is calculated by applying propagation of uncertainty theory in accordance with Taylor [39], accounting for the biases of surface pressure, velocity and density measurements. The bias limit of the surface pressures is taken as the maximum error from the static calibration (±16 Pa) whilst the bias limits of velocity and density measurements are respectively taken as and calculated from manufacturer specifications. The random uncertainty in pressure coefficients is estimated as twice the standard error of the mean, assuming mean values from each run of the experiment are normally distributed and considering a confidence level of 95% [39].

The ensemble mean surface pressure coefficients are used to calculate the drag coefficients through integration of pressure over a discretised geometry of the vehicle surface. Discretised areas are formed by creating a polygon centred on each tapping point, extending halfway to the neighbouring tapping point or to the surface edge. The overall load coefficients can be defined as [29, 34],

$$C_X = \frac{F_X}{\frac{1}{2}\rho V_{plat}^2 A_{ref}} = -\frac{\sum_i \overline{C_{P_i}} A_i (\mathbf{n}_i \cdot \mathbf{x})}{A_{ref}} \tag{7}$$

where F_X is the ensemble average drag force and A_{ref} is taken as the entire projected area of the lorry normal to the direction in which the force acts, equal to 8.0 m^2 at full-scale. $\overline{C_{P_i}}$ is the ensemble average pressure coefficient for each pressure tapping i associated with discretised area A_i and the normal unit vector n_i. The negative sign on the leftmost side is included to give positive drag coefficients within the adopted coordinate system.

The drag was estimated from 12 pressure taps: 5 on the cab front, 2 on the front of the box-section and 5 on the rear. Due to experimental constraints, this number of pressure taps is less than would be desirable to accurately compute drag. The reliability of the drag estimates is assessed by comparing the values obtained for a single lorry to values obtained by other researchers. The data will also be used to validate/calibrate CFD calculations, from which a more accurate estimate of C_X can be calculated, in a separate paper.

The uncertainty in the drag coefficient is calculated by applying propagation of uncertainty theory in accordance with Taylor [39], under the assumption that the computed loads for each discretised area are independent. This accounts for the total uncertainty in the mean C_P for each tap. It should be noted that the uncertainty estimate for C_X may be less than

the true error due to the low resolution of pressure taps, neglected surface-friction contributions and the assumption that the pressure is uniform across each discretised area [40]. The maximum uncertainty is ±0.06 for lorry 1 and ±0.04 for all lorries behind.

3 Results and Discussion

3.1 Slipstream development

The aerodynamic flow development at the side of the lorry platoon, for the different vehicle spacings examined, is shown in figures 3 and 4. The non-zero windspeeds before the platoon approaches (for say $\tau < 1$) are assumed to be zero. The measured non-zero values are attributed to the greater uncertainty of velocity measurements with a magnitude lower than 2 m/s ($U < 0.08$). The flow is characterised by a thick boundary layer type development which exhibits some dependence on the spacing between lorries. At the beginning of the platoon as the first lorry passes there is a small peak in velocity for measurements close to the lorry side. Whereas, for measurements further from the lorry side the peak is less clear and is entrained within the rapid boundary layer development. High velocity magnitudes are observed for measuring positions close to the ground plane, thought to be due to the confinement of the flow by the ground plane; this observation is consistent for all measuring positions from the lorry side. Interestingly, the highest measuring position at 3 m exhibits higher velocity magnitudes than the 1.6 m position, again an observation consistent for all lateral measuring positions. A series of velocity peaks in the boundary layer development, seen for a measuring height 3 m but not 1.6 m, relate to positions close to the front of each lorry. The 3 m position is close in height to the top edges of the lorry, thought to create regions of large flow separation inducing the subsequent peaks in velocity magnitude. The measuring positions above the lorry platoon roof (not shown) exhibit lower velocity magnitudes in relation to similar distances away from the lorry surface measured at the lorry side. This is consistent with previous studies on freight trains [33] and goes someway to explaining the larger magnitudes measured at height 3 m for positions at the lorry side, where flow above the roof and at the lorry side converge.

Soper et al. [33] showed that as containers were removed from a freight train and spaces increased between those remaining that the magnitude of slipstream velocities within the boundary layer increased and were punctuated with a series of velocity peaks relating to the front edge of each container where a large flow separation occurs. This case is similar to the platoon of lorries with the larger spacing between vehicles. For the case of lots of small spaces between containers, similar to the short vehicle spacing in the platoon, Soper et al. [33] found rapid boundary development was created by lots of smaller turbulent structures created as the larger flow separations merge into the wake of the previous structure. Velocity magnitudes were shown to reach lower values than for the larger spacing, as shown in figures 3 and 4 for the platoon [33].
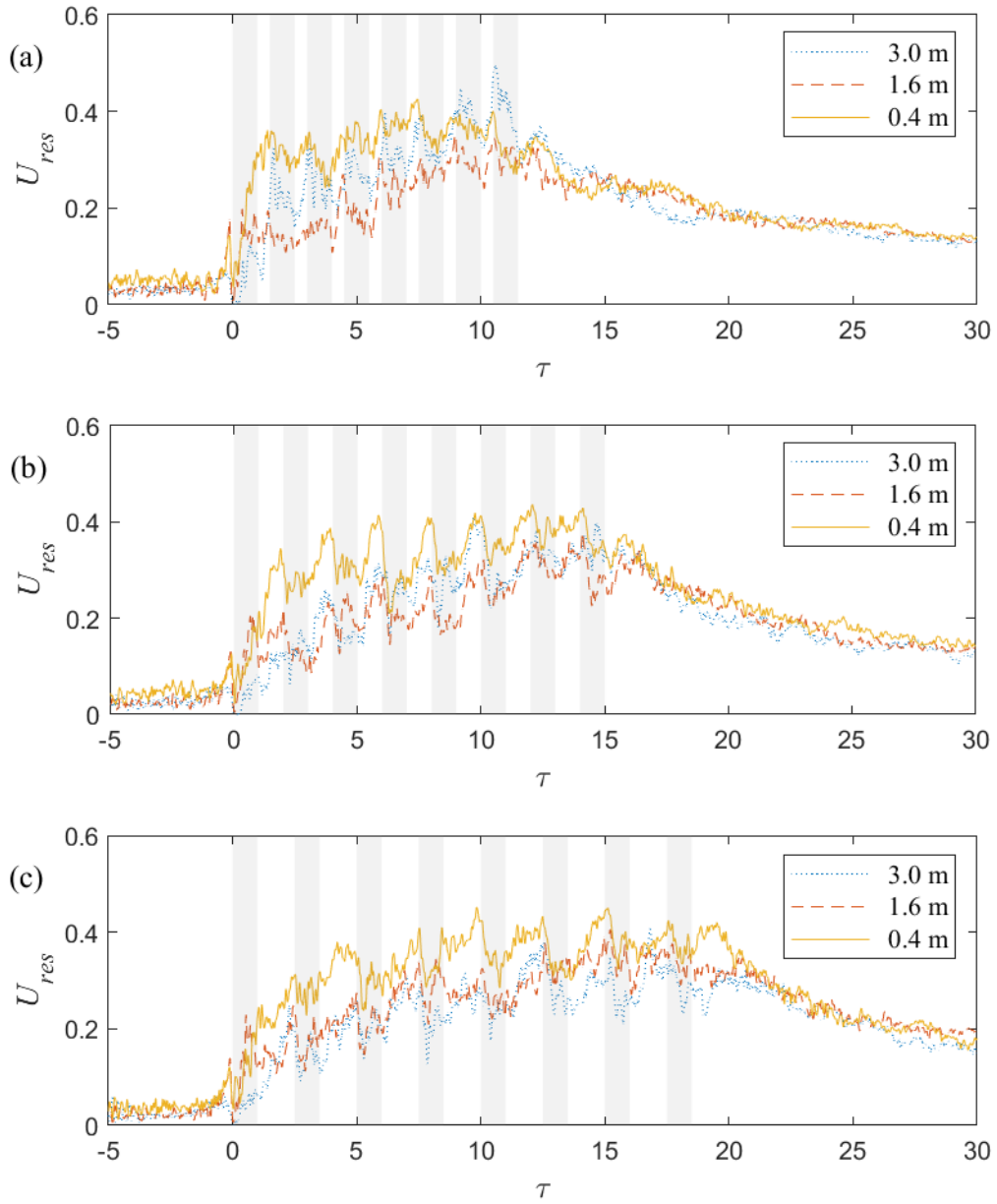
Figure 3: Normalised horizontal velocity as a function of normalised time, 0.5 m from the lorry sides, at various heights above ground level. The spacing between vehicles is: (a) 0.5*L*, (b) 1.0*L* and (c) 1.5*L*.
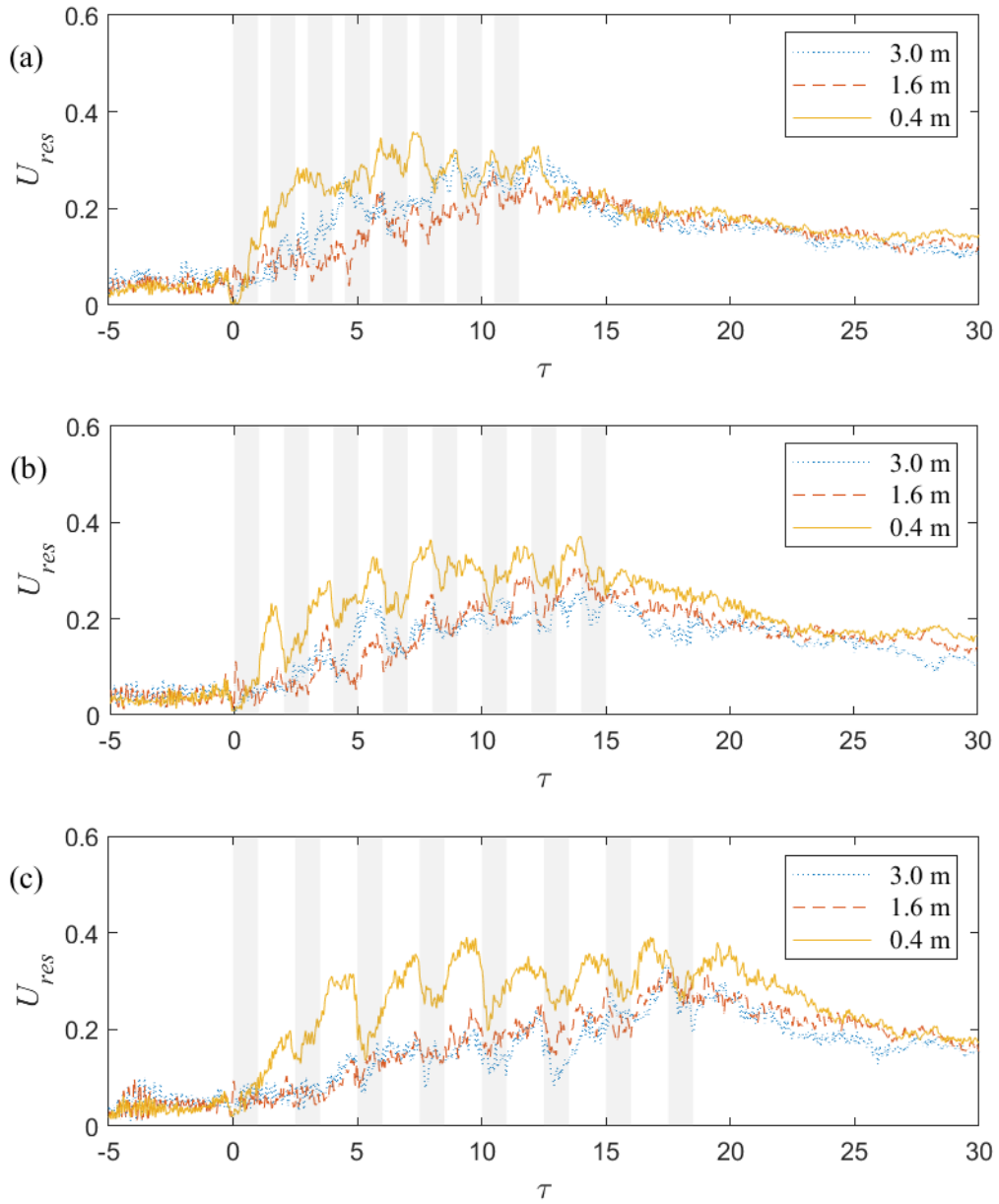
Figure 4: Normalised horizontal velocity as a function of normalised time, 1.0 m from the lorry sides, at various heights above ground level. The spacing between vehicles is: (a) 0.5*L*, (b) 1.0*L* and (c) 1.5*L*.

Figure 5 shows individual runs of the normalised horizontal velocity, as well as the ensemble mean and standard deviation, as a function of normalised time for a single measurement position to the side the lorries. There is a large degree of variability both within a single run over time and between runs. The latter leads to large ensemble standard deviations in relation to the means.
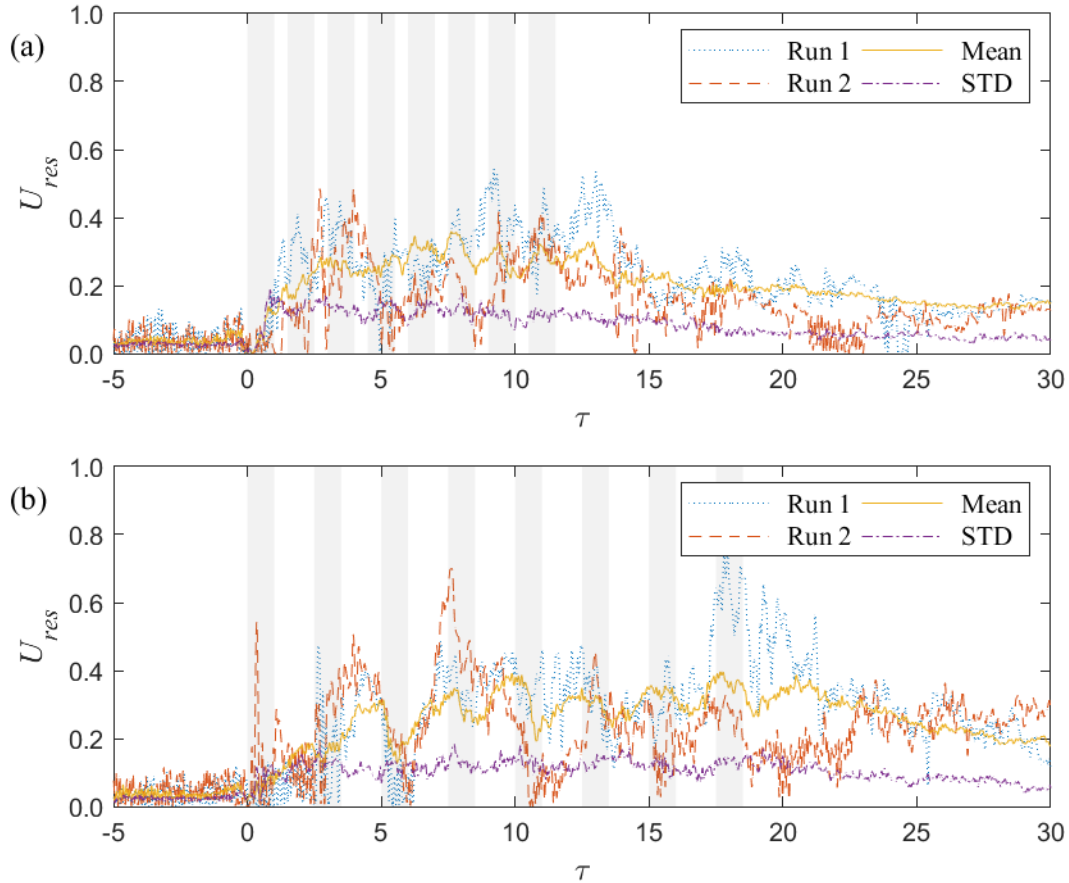
Figure 5: Normalised horizontal velocity as a function of normalised time, 0.4 m above ground level, 1.0 m from the lorry side. Selected runs and the ensemble mean and standard deviation (STD) of all 20 runs for (a) 0.5L spacing and (b) 1.5L spacing.

Figures 6 and 7 show the longitudinal turbulence intensities at different positions to the side of the lorries. It is worth noting that the data for the position 1.0 m from the lorry sides presented in figures 6c and 7c are also presented in Figures 5a and 5b respectively. It is clear that as the boundary layer flow along the platoon increases so does the level of turbulence. The flow for all spacings can be characterised as highly turbulent, with high levels of small-scale turbulent structures, as well as large structures emanating from leading edge separations. A clear observation from figures 3-7 is the variability of the results presented, even within the ensemble averages. The bluff nature of the box lorries leads to large flow separations from the cab and leading box edges which contribute to the large velocity peaks observed in the ensemble flow.
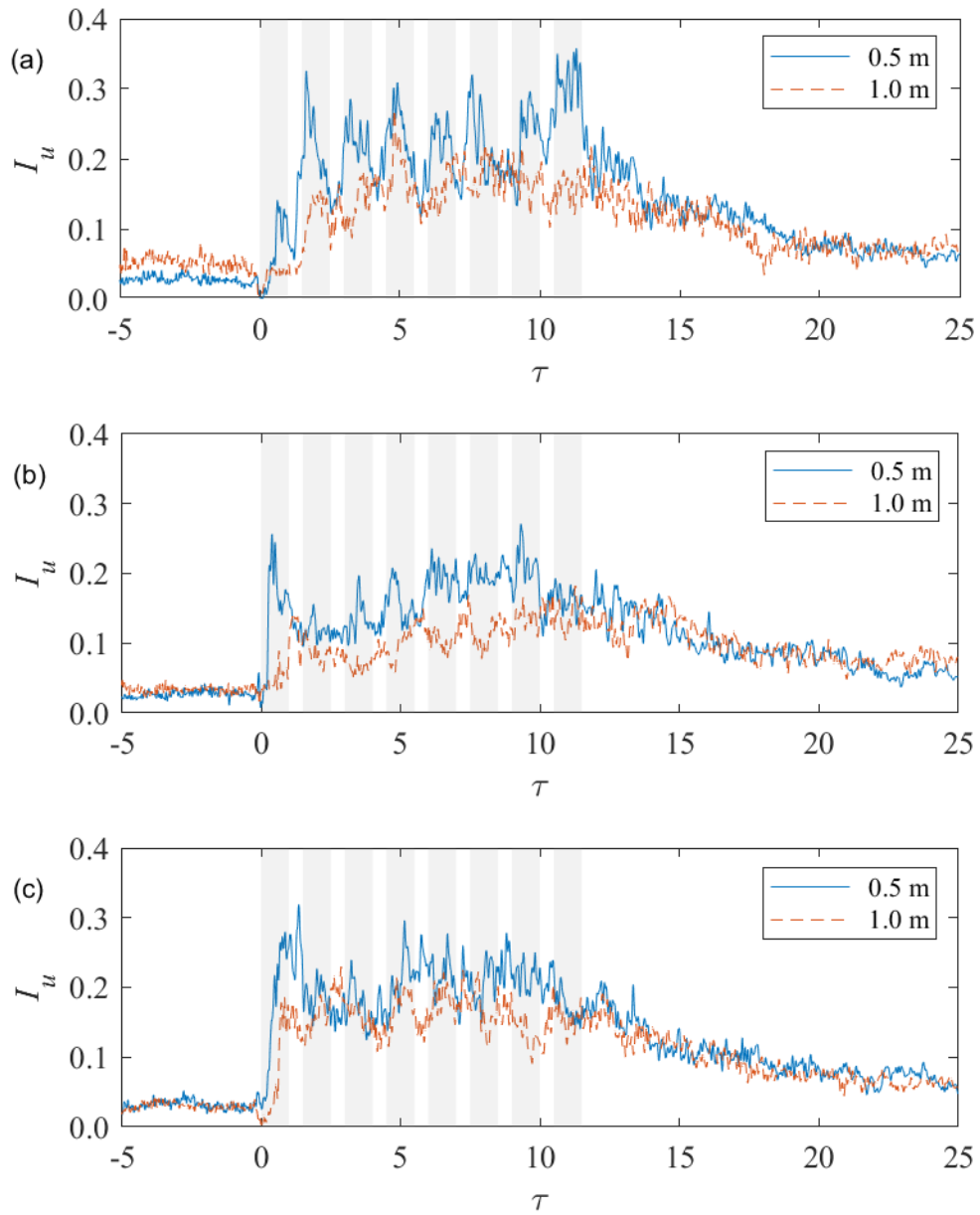
Figure 6: Longitudinal turbulence intensity 0.5 m and 1.0 m from the lorry side for a vehicle spacing of 0.5*L*. The height above ground level is: (a) 3.0 m, (b) 1.6 m and (c) 0.4 m.
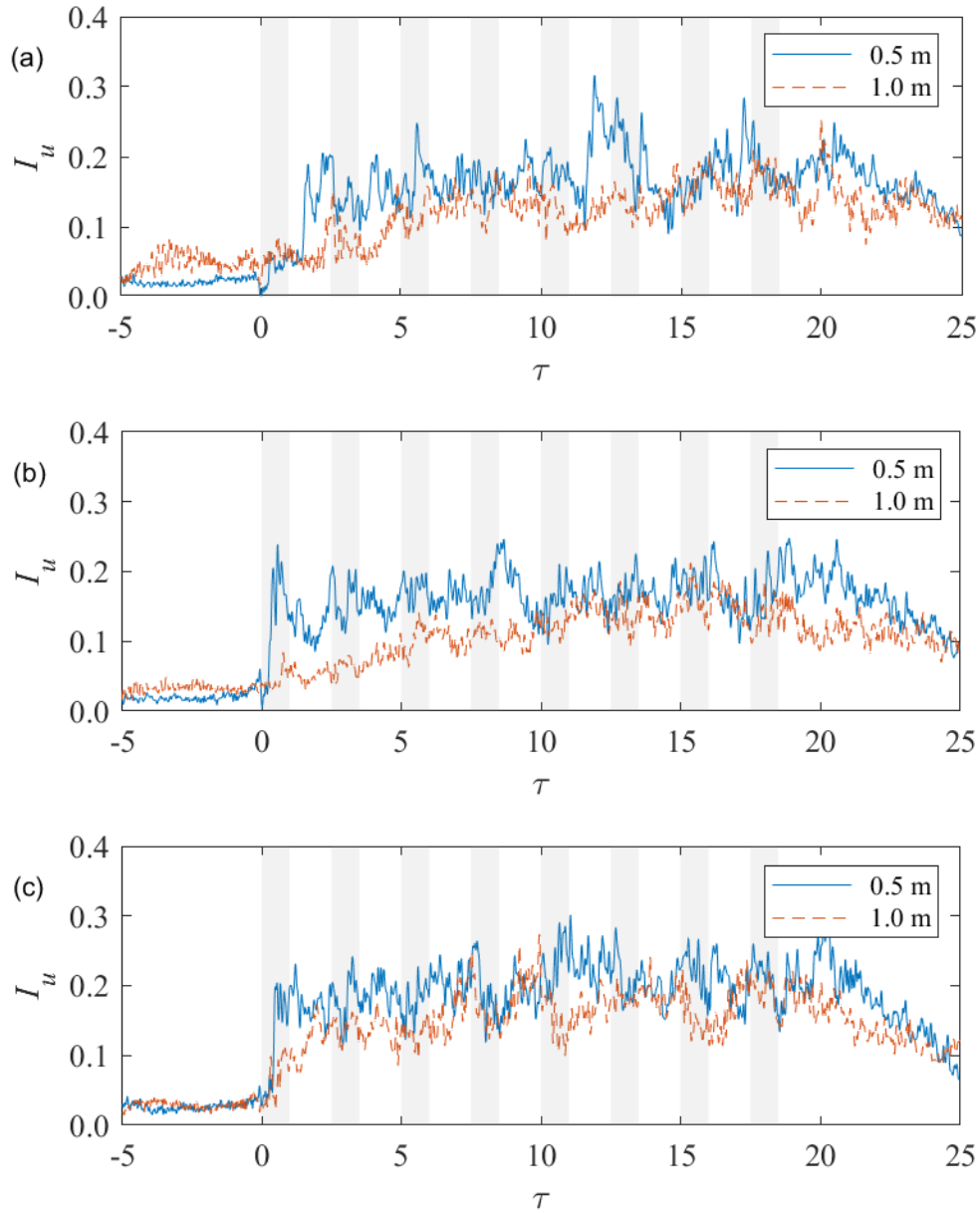
Figure 7: Longitudinal turbulence intensity 0.5 m and 1.0 m from the lorry side for a vehicle spacing of 1.5L. The height above ground level is: (a) 3.0 m, (b) 1.6 m and (c) 0.4 m.

Results for coefficient of pressure within the flow also exhibit similar development between the platoon and a freight train as shown in figure 8. The characteristic change in pressure about the nose of a vehicle with a positive then negative peak is observed for each vehicle in the platoon. Along the vehicle side the pressure stabilises before a positive peak is observed at the back of the vehicle, which for the short formation, leads directly into the positive peak at the nose of the following vehicle. This results in a distinctive pressure profile where the vehicles act as a platoon aerodynamically. In contrast, for the larger spacing, similar pressure traces are observed for each vehicle with higher peaks and a lower frequency, $f \approx V_{plat}/(L+s)$, where s is the vehicle spacing.
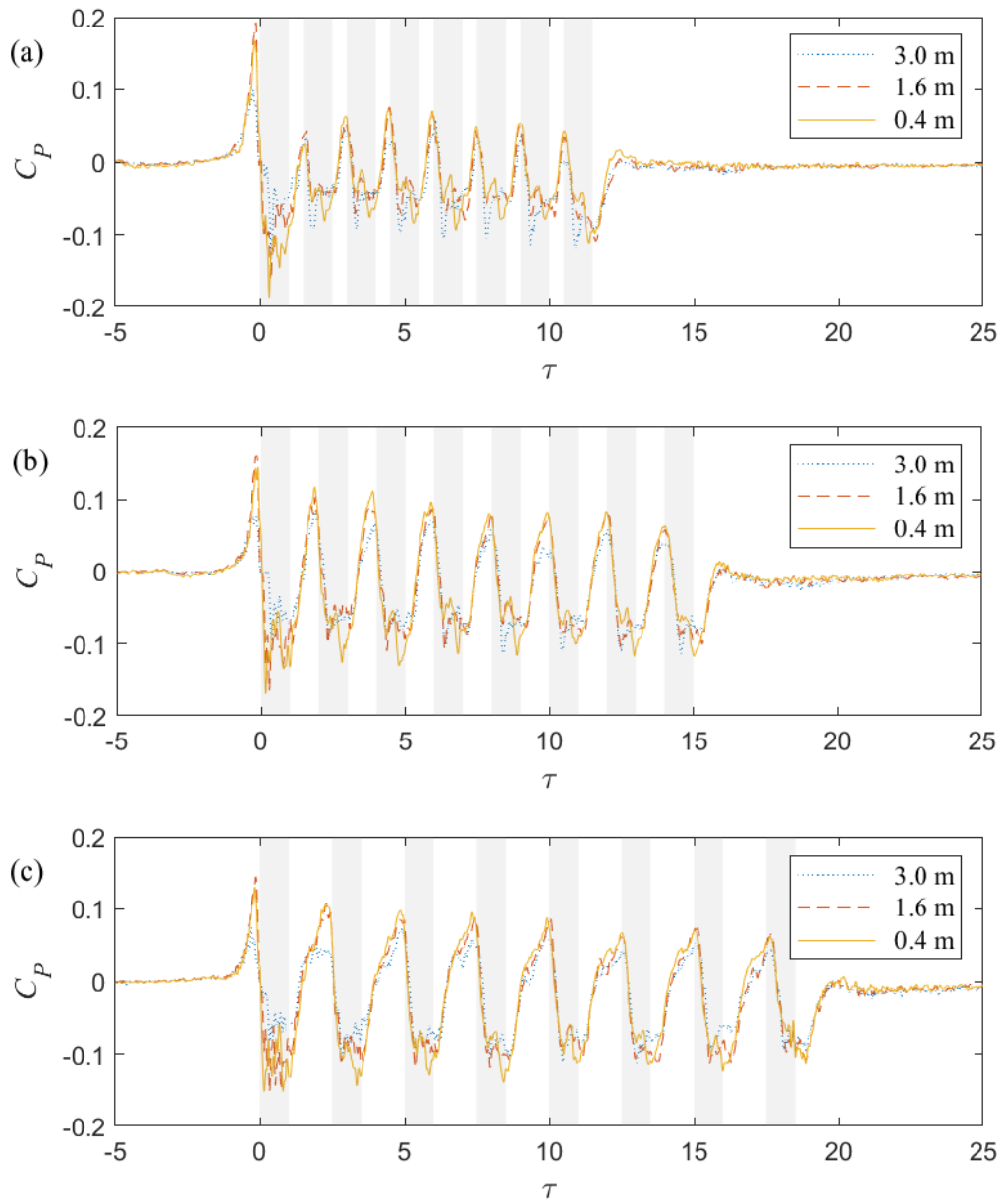
Figure 8: Pressure coefficient as a function of normalised time, 0.5 m from the lorry sides, at various heights above ground level. The spacing between vehicles is: (a) 0.5*L*, (b) 1.0*L* and (c) 1.5*L*.

As discussed, these findings show similar flow development to that characterised previously by Soper et al. [33] for container freight trains with various spacing between container loading configurations. Indeed, visually a platoon of lorries is similar to a container freight train; simply a series of cuboids moving linearly in a consistent formation, although somewhat ironic as road vehicles took freight traffic away from the railways [41]. The difference in shape between an individual lorry and a single container seems to have little effect on qualitative trends in the velocity and pressure to the side of the vehicle suggesting that much can be understood about the aerodynamics of platoons by considering the aerodynamics of freight trains. This finding is particularly important in light of a series of high-profile incidents involving trains travelling through stations. At Twyford, a wheelchair containing a passenger was sucked into the side of a freight train, before rebounding leaving the passenger with only minor injuries [42]. At Nuneaton, a pushchair containing only shopping was sucked against the side of a passing freight train and destroyed and a similar incident occurred at Maidenhead [43-44]. Thus, the similarity between the airflows surrounding freight trains and lorry platoons should raise concern that such instabilities could occur with other road users (e.g. motorcyclists) close to a platoon of vehicles.

3.2 Mean surface pressure

Figure 9 compares the distribution of mean surface pressure coefficients on a single lorry to full-scale measurements, with a moving lorry, from Quinn et al. [29] at a Reynolds number approximately an order of magnitude higher. The full- and model-scale experiments show similar trends, namely a high suction near the top of the box-section which decreases with increasing distance along the lorry length on the lateral centreline and around the sides as shown in figures 9b and 9a respectively. However, the model-scale C_P typically has a much lower magnitude. This could be due to a Reynolds number effect on flow reattachment which leads to low pressures over the top and sides of a bluff body. A similar result was obtained previously by Hoxey et al. [45] who compared full-scale and wind tunnel surface pressures coefficients on a cube and found that, in a headwind, there was close agreement on the windward face but larger suctions over the roof and side-wall at full-scale. At a 45° yaw angle, this was no longer the case and close agreement was obtained between measurements at both scales, attributed to a similar Reynolds number effect though the authors noted that more evidence was needed to confirm this. An alternative explanation for the discrepancy between the model and full-scale measurements is that the low values of pressure coefficient on the top and side faces were artificially created by the analysis methodology that was used by Quinn et al. [29]. The data were grouped into quite large yaw angle bins and thus effectively included data in the analysis where there was a very wide range of pressure coefficient as the yaw angle varied, resulting in the anomalous low values. Turbulence levels in the wind and the interactions between the wind and slipstream around the vehicle may also have been factors. Regardless of the reason for the discrepancy, the important aspect is the agreement between the general trends of the full- and model- scale data.

The results for a single lorry are also compared to those for the downwind lorry at 14L spacing and for the front lorry in the sparsest platoon in figure 9. Both these sets of measurements agree with the single lorry measurements to within uncertainty at all measured locations. This suggests that for a vehicle spacing as large as 1.5L, C_P on the front lorry is largely

unaffected by the trailing lorries even towards the rear of the vehicle. Only a single data point is available on a windward face at full-scale (on the box front), but this is in close agreement with the available model-scale measurements at this location (1.5*L* and 14*L*), consistent with both of the above explanations for the discrepancies between scales of the top and side pressures.
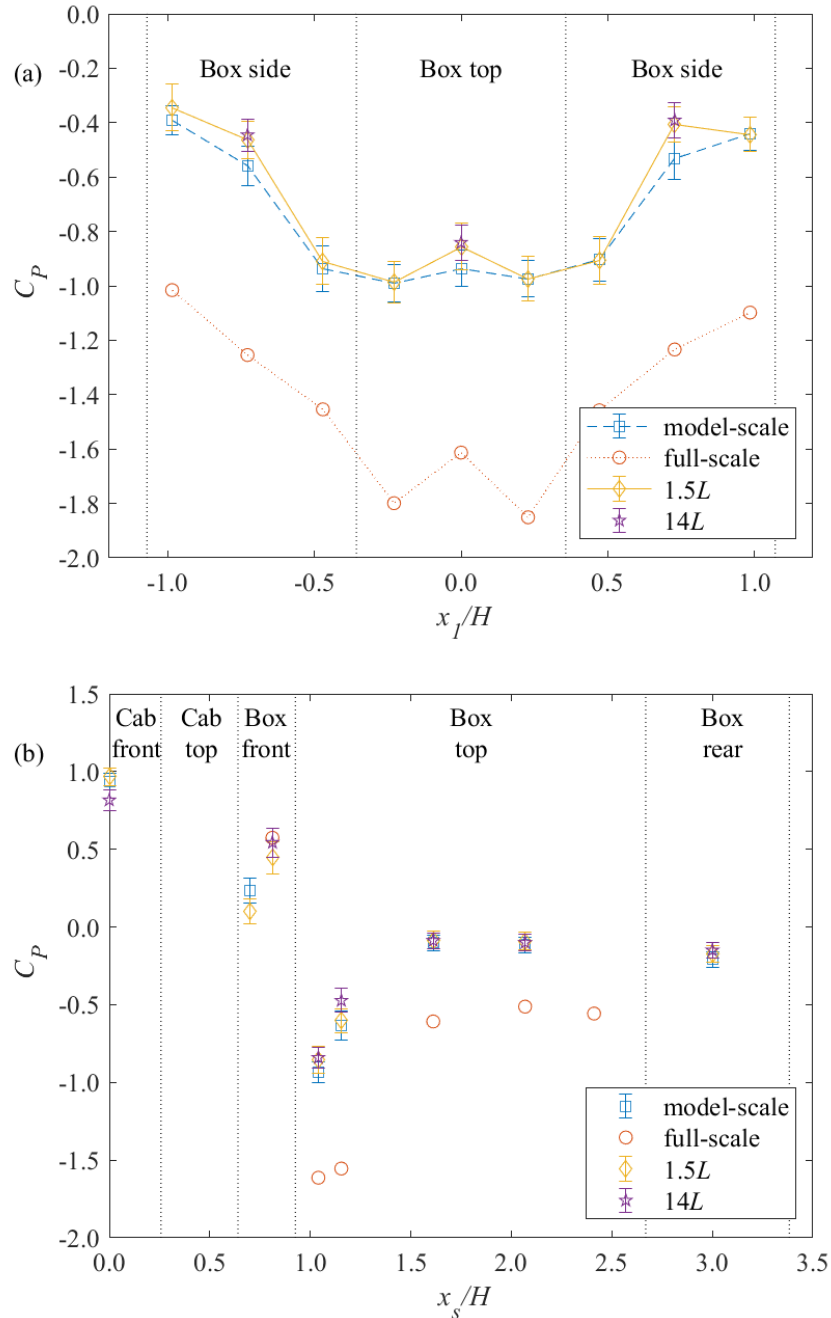

Figure 9: Mean surface pressure coefficients (a) around the front loop through the lorry box-section and (b) around a slice through the symmetry plane. "Model-scale" denotes the upwind lorry in a 2-vehicle platoon at 14*L* spacing and "14*L*" denotes the downwind lorry. "Full-scale" data are from Quinn et al. [29]. "1.5*L*" is lorry 1 in a platoon at 1.5*L* spacing.

21

Figure 10 shows the mean pressure coefficients around the front loop of the box-section for lorries in a platoon at 0.5L spacing. The pressure is particularly low at the lateral centreline of the box top which is just past the front edge where the flow separates. This is far more pronounced for the first lorry, which is subject to a higher incoming flow speed. The pressure on lorry 1 closely resembles that of an isolated lorry (figure 9a) suggesting the trailing lorries have little impact on pressures near the front of lorry 1, even for spacings as small as 0.5L. The downwind lorries are shielded from high velocity flow very effectively, leading to substantial decrease in pressure magnitudes towards the rear of the platoon, particularly over the top of the box-section. The pressure results plateau further back into the platoon and is consistently equal to within uncertainty for lorries 5 and 8. A similar trend is observed at the larger spacings, but the increase in pressure towards the rear of the platoon is less pronounced.
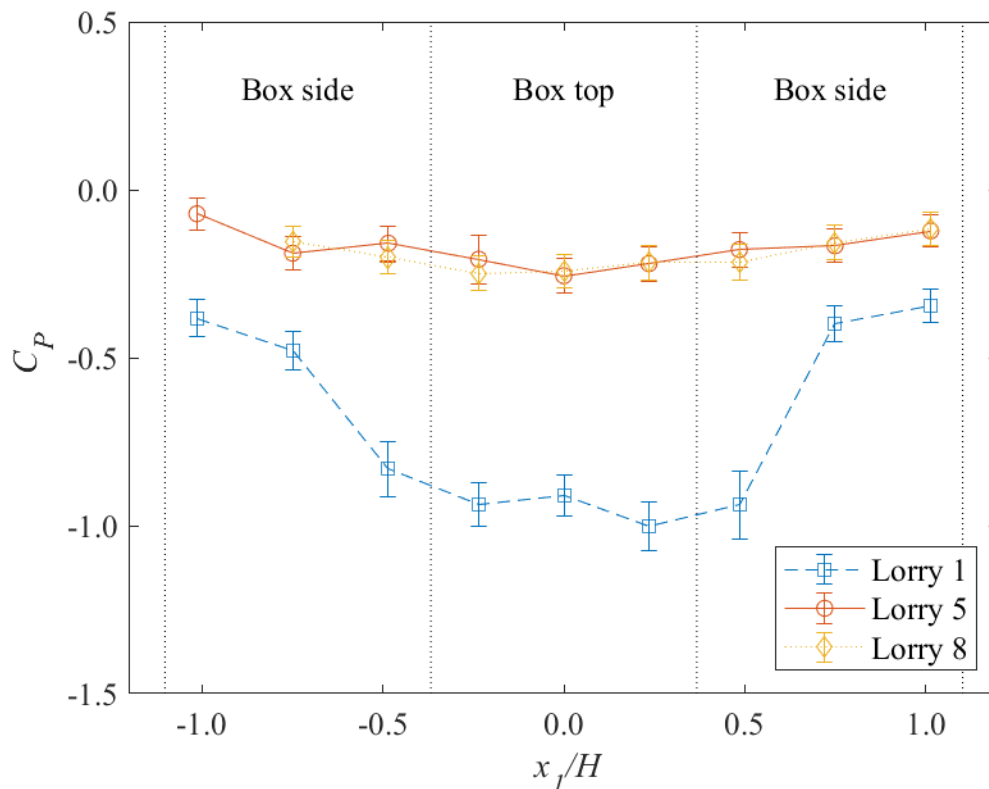

Figure 10: Mean pressure coefficient vs. position around the front loop of the box-section for the platoon with 0.5L spacing between lorries.

The mean surface pressure coefficients on lorries 1, 5 and 8, around the symmetry plane, at spacings of 0.5L and 1.5L spacing are shown in figure 11Figure . At all measured locations, lorries 5 and 8 are shielded very effectively leading to lower pressure magnitudes than on lorry 1 (or equal to within uncertainty) but C_P plateaus towards the rear of the platoon, with values constant to within uncertainty for lorries 5 and 8 (at both spacings). Similarly, as shielding is more effective at closer spacing, the magnitude of the surface pressure on lorries 5 and 8 is either much lower at the closest spacing or equal to within uncertainty across both spacings.
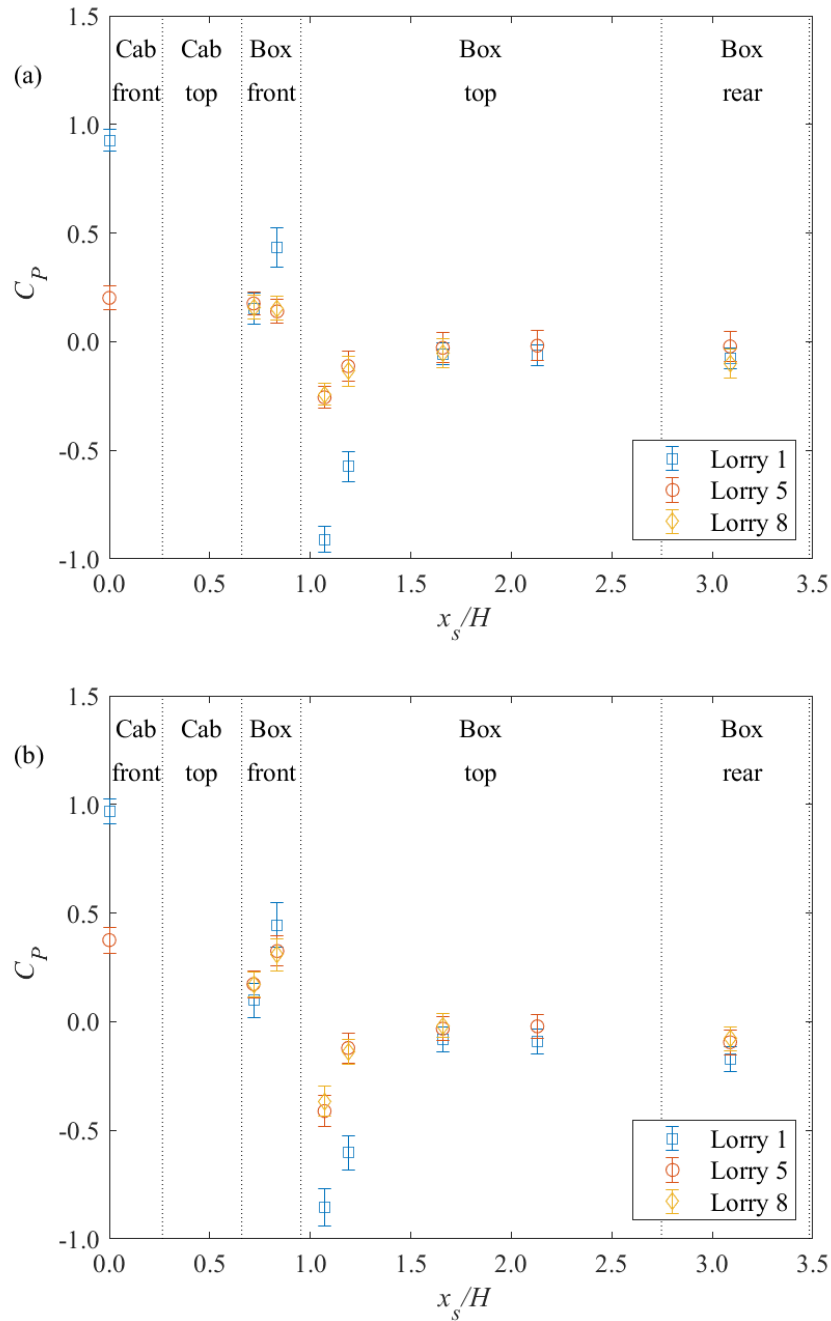
Figure 11: Mean surface pressure coefficient vs. position around a slice through the symmetry plane of the lorries for (a) 0.5L and (b) 1.5L vehicle spacing.

The peak surface pressure occurs on the front of the cab. For the first lorry, which is unshielded, this pressure is close to the dynamic pressure and is within uncertainty for the two spacings. In fact, surface pressures on lorry 1 across both spacings are within uncertainty at all locations, again suggesting that the trailing lorries have little effect on the surface pressures on the front lorry, even towards the rear of the vehicle and even in the most closely spaced

platoon. Shielding has a greater impact on pressures at the front of the lorries, leading to a significant decrease in the cab front pressure between lorries 1 and 5, which is more pronounced at the closest spacing. On the front of the box-section, as one may anticipate, the pressure typically increases with distance above the front face of the cab, where the flow stagnates, towards a larger value nearer to the top edge. The exception to this is for the downwind lorries at $0.5L$ spacing where the pressure remains almost constant at a relatively low value over the front face of the box. This can be ascribed to the fact that at close spacing the flow has little time to recover in the wake of each vehicle and as a result the incoming flow speed is particularly low at the height of the box-section of the downwind vehicles, leading to lower surface pressures. After the high pressure near the top edge of the front of the box-section, there is a steep pressure drop over the top edge where the flow separates. This is more pronounced for the first lorry, which is subject to a higher incoming flow speed. The lowest surface pressure coefficients are consistently measured at this location and are of the order of -1 for the front vehicle. There are lower pressure magnitudes for the non-leading lorries, at $0.5L$ spacing than at $1.5L$ spacing due to greater shielding, at the positions high on the box front and at the front of the box top. Towards the rear of the box-section, where the flow recovers to some extent, and on the rear face the surface pressures are constant to within uncertainty for all three lorries at a given spacing, and for a given lorry at each spacing. One may have anticipated that stagnation on the front of a downwind vehicle would tend to raise the rear pressure of the lorry immediately upwind. Indeed, although the mean pressure coefficients on the rear of lorry 1 at $0.5L$ and $1.5L$ spacing just fall within their combined uncertainties, there is an increase in pressure on the rear face at $0.5L$ spacing when compared to the isolated lorry (figure 9b).

3.3 Mean drag

It is worth reiterating that, due to experimental constraints, the number of pressure taps available to compute C_X is limited. The primary purpose of the surface pressure measurements was to provide C_P values at indicative locations to validate/calibrate CFD models. Nevertheless, as the same tap locations are used for each vehicle and spacing the computed C_X is still a useful measure of the integrated pressure drop which is sufficient to make comparisons between vehicles in different positions and between spacings. To assess the reliability of C_X estimates the value obtained for a single vehicle can be compared to previous research, where wind tunnel approaches have been well validated. Drag coefficients for a single lorry and for the front lorry in each platoon are shown in Table 2. For the single lorry C_X is 0.63 ± 0.06 which agrees with the value measured with a 6-component dynamometric balance on the same vehicle at 1/10th scale, in a wind tunnel test, by Cheli et al. [31] and with the LES results from Patel et al [32]. These studies used a more sophisticated model geometry which didn't remove the fine-scale elements. The close agreement therefore suggests that the tendency of suction at the edges of the front faces to increase C_X is compensated for by the combined effects of friction on the vehicle sides and the pressure drop across fine-scale elements such as wing mirrors. Nevertheless, the agreement gives confidence that the number of pressure taps in the present study is sufficient to provide an indicator of C_X and validates the assumption that the simplified geometry in this study is reasonable to determine drag. The measured drag coefficient is also within uncertainty of the wind tunnel tests by Allan [46] on a simplified tractor-trailer model

comprising only of two tandem boxes, with rounded corners, with comparable scaled dimensions to the present study. The drag on the front lorry in each platoon is also shown in Table 2. These values agree to within uncertainty with the single lorry measurements. However, there is a reduction in drag for the front lorry at 0.5L spacing when compared to that at 1.5L spacing.

Vehicle spacing	Method	C_X
Single lorry	Moving model	0.63 ± 0.06
Single lorry*	Moving model	0.62 ± 0.05
Single lorry [31]	Wind tunnel	0.66 ± 0.09
Single lorry [32]	LES	0.61
Two tandem box model [46]	Wind tunnel	0.59
0.5L	Moving model	0.55 ± 0.05
1.0L	Moving model	0.64 ± 0.06
1.5L	Moving model	0.66 ± 0.04

Table 2: Drag coefficients on a single lorry and the front lorry in a platoon.
Values from Cheli et al. [31], Patel et al. [32] and Allan [46] have been adjusted, so that they are based on the entire projected area normal to flow, as in the present study.
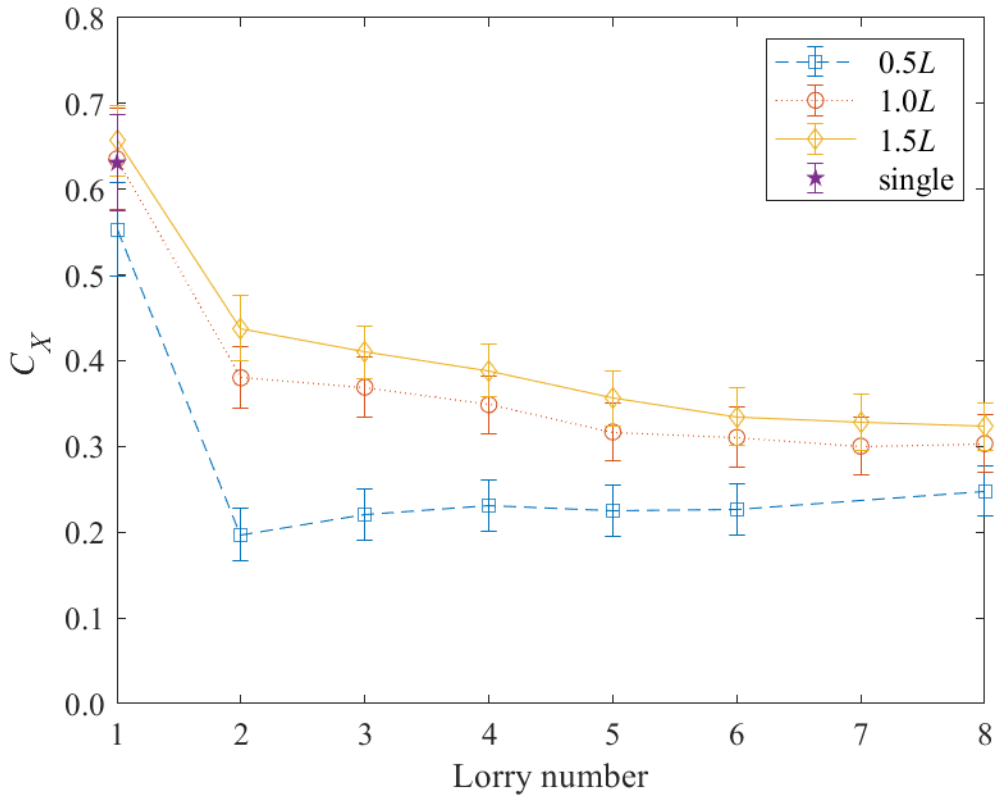*Downstream lorry at large spacing of 14L.

Figure 12: Drag coefficients on each lorry in a platoon

Figure 12 shows the drag coefficients of a single lorry and each lorry in a platoon. At all three spacings, the drag coefficient on the downwind lorries (i.e. 2 to 8) is significantly lower than that of the single lorry. The results also show a reduction in drag with vehicle spacing. Drag coefficients, for a given lorry, at spacings of 1.0*L* and 1.5*L* fall within uncertainty but there is a marked reduction in drag when the spacing is reduced to 0.5*L*. This suggests that when the vehicles are relatively far apart, a reduction in spacing causes at most a small reduction in drag but as the spacing is reduced to below 1.0*L*, the reduction is far more rapid. The largest change in drag, at a given spacing, occurs between the first and second lorries, presumably due to the largest change in approach velocity. At the two largest spacings, the drag tends to decrease on lorries towards the rear of the platoon, as the incoming flow velocity is reduced further behind each lorry. At the closest spacing however, C_X is constant to within uncertainty from the second vehicle onwards.
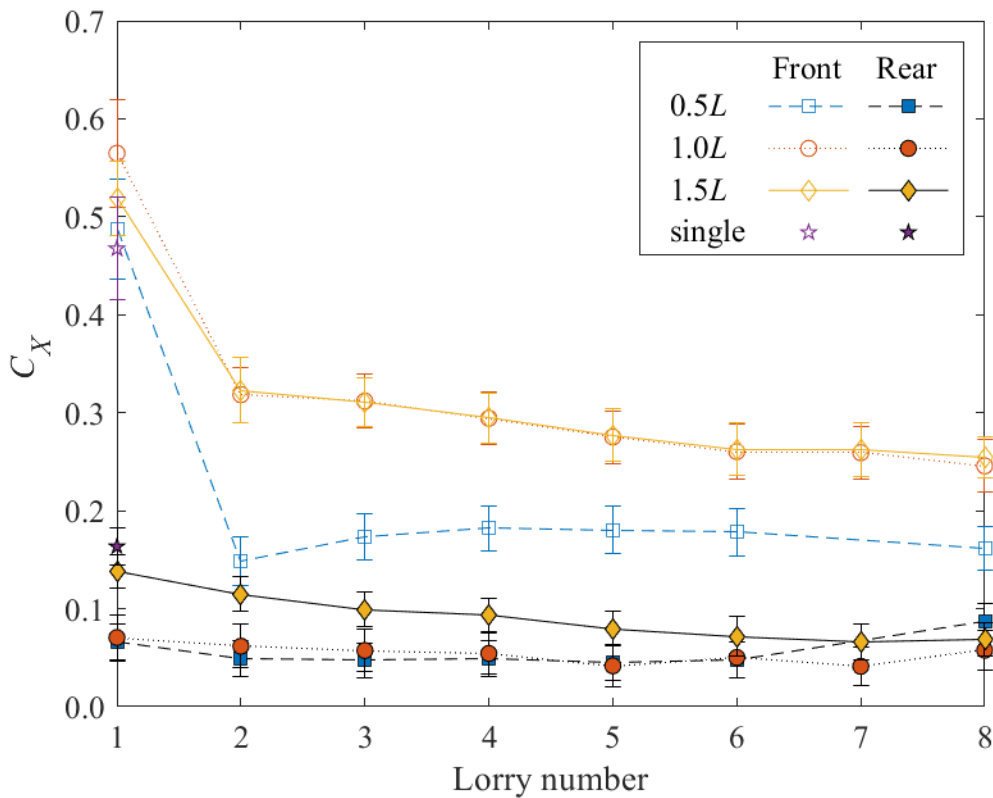

Figure 13: The contributions of front and rear faces to lorry drag coefficients.

Figure 13 shows the contribution of the front (cab and box) and rear faces to C_X. For all lorries and platoon configurations, a large majority of the drag arises from high pressures on the front face. For lorry 1, which is unshielded, the front contribution at all spacings remains within uncertainty of the value for the single lorry. The rear contribution is within uncertainty of the single lorry at a spacing of 1.5*L*, but as the spacing is reduced to 1.0*L*, stagnation on the front of lorry 2 raises the rear pressure, reducing the rear contribution to C_X. At a given spacing, the rear face contribution on the first and second lorries are within uncertainty. Hence, the

large reduction in drag on the second vehicle, arising from a large decrease in the front face pressures, which is predominantly set by shielding from lorry 1. Even at the largest spacing, the reduction in the front face contribution between the first and second vehicles is significant, suggesting that experiments modelling the forces on road vehicles should often consider the influence of an upstream vehicle, as a pair of vehicles may travel at comparable spacings for long distances in practical situations, e.g. on busy motorways, even if those vehicles not deliberately platooning. To this end, a wake generator (a short, bluff body designed to recreate the wake flow from the leading vehicle) could be used in wind tunnel studies, to maximise the length of the test section available to the model without the need to reduce the scale [47-48].

The front contribution to drag on a given lorry is within uncertainty at the two *largest* spacings and is much lower for 0.5L (or within uncertainty in the case of lorry 1). However, the rear contribution is within uncertainty at the two *smallest* spacings and is either higher or within uncertainty for 1.5L, depending on the lorry position. This explains why any reduction in drag for lorries 2 to 8, with a reduction in spacing, becomes more rapid as the spacing is reduced i.e. because there is a much larger decrease in the front contribution to drag, as the spacing is reduced from 1.5L to 0.5L, than there is in the rear contribution.

The mean drag coefficient across the entire platoon is shown in table 3. Data for lorry 7 at 0.5L spacing are unavailable due to experimental difficulties, so C_x has been estimated as the average value from lorries 6 and 8. Even at the largest spacing of 1.5L the reduction in mean drag relative to isolated lorries is significant (between 24% and 46%). At 0.5L spacing, the drag is reduced by at least 48% (accounting for uncertainties) demonstrating that significant aerodynamic benefits can be achieved for a typical lorry due to platooning.

Spacing	0.5L	1.0L	1.5L	Single
C_X	0.27 ± 0.03	0.37 ± 0.04	0.40 ± 0.03	0.63 ± 0.06
Reduction (%)	48 - 66	29 - 52	24 - 46	0

Table 3: Mean drag coefficient across all lorries in a platoon and the reduction relative to a single lorry.

Figure 14 shows the drag reduction across all lorries in platoon formation, relative to the same number of lorries travelling in isolation, as a function of the vehicle spacing. This is compared to wind tunnel data for 2, 3 and 4 car platoons from Zabat et al. [15]. The drag reduction for 8 cars has also been estimated by extrapolating their data, via linear regression of the drag ratio against the reciprocal of the number of vehicles (1/1, 1/2, 1/3 and 1/4), as suggested by Zabat et al. [15]. The best estimates of the drag reduction for lorries show a similar general trend to the cars, namely a decrease in the drag reduction with increased spacing, which declines less rapidly when the spacing is relatively large (except at spacings smaller than considered in experiments in the present study). There is a much larger drag reduction for the lorries than the cars as the bluffer lorry shape shields the downwind vehicles more effectively. Nevertheless, as the drag coefficient of a single car (0.33) is much lower than a lorry, the mean drag coefficients are much larger for the bluffer body e.g. 0.37 ± 0.04 and 0.25 for platoons of eight lorries and lorries respectively at 0.5L spacing.
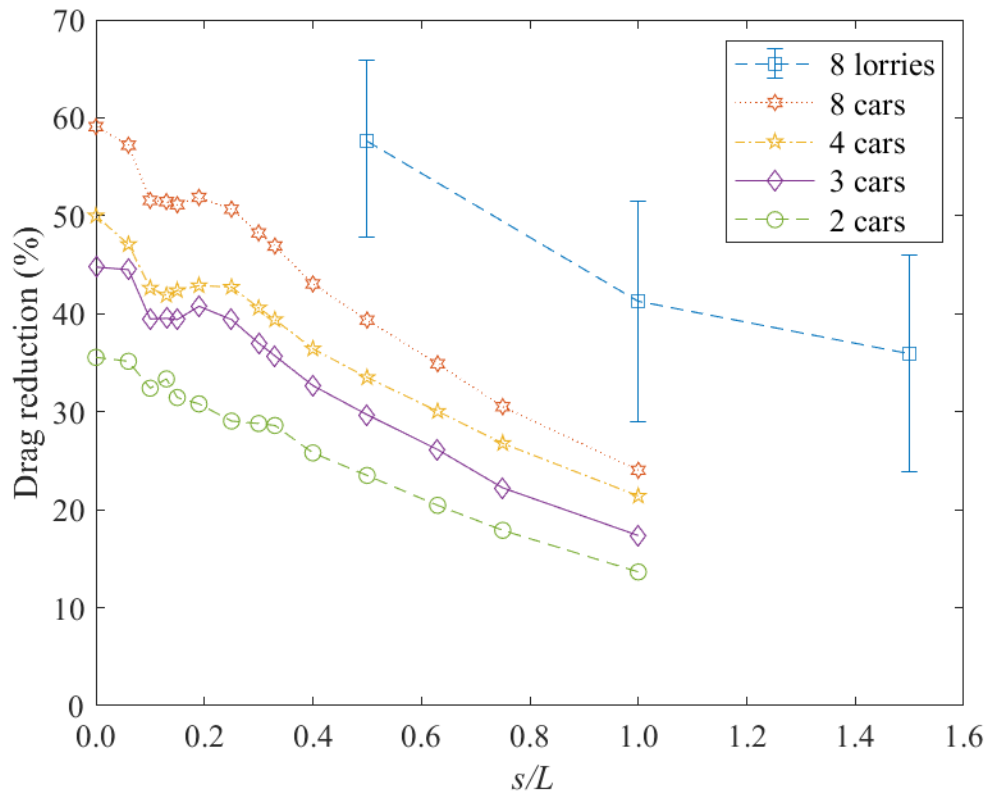
Figure 14: Drag reduction across all lorries in the platoon vs. spacing ratio for lorries (present study) and cars [15].

4 Conclusions

Novel moving model vehicle experiments, at 1/20th scale, have been conducted to examine the aerodynamics of a platoon of typical commercial lorries. The number of vehicles (eight), speed (25 m/s) and spacing (half to one-and-a-half vehicle lengths), are appropriate for autonomous road vehicles. The main findings can be summarised as follows:

- The flow surrounding the lorries is characterised by a thick boundary layer development with peaks in velocity and pressure which correspond to the front of each lorry. As the spacing increases, peak velocities reach higher magnitudes. The highest velocities occur at low heights, attributed to the confinement of the flow by the ground plane.

- The slipstream behaviour is similar qualitatively to that found from previous research on freight trains. This is particularly important in light of a series of incidents where wheel/pushchairs have been drawn into the side of the moving trains. The clear similarities in aerodynamic flows, should raise concern that this could also occur with other road users (e.g. motorcyclists) near platoons.

28

- Surface pressures on a single lorry show similar trends to full-scale measurements from previous research, namely high suctions near the front edge on the top of the box-section which decrease along the lorry length on the lateral centreline and around the sides.

- The downwind lorries are shielded very effectively by those upstream, leading to a substantial decrease in pressure magnitudes on lorries towards the rear of the platoon. However, the pressure at a given position (and drag) plateaus reaching near constant values for the fifth and eighth lorries. As shielding is more effective at close spacing, the pressure magnitude is either much lower at the closest spacing or equal to within uncertainty across spacings.

- The drag coefficient of an isolated lorry is 0.63 ± 0.06, in agreement with previous research. The drag coefficient of the front lorry in a platoon falls within uncertainty of the isolated lorry and is consistently lower for the downwind lorries (i.e. 2 to 8) over the conditions considered. There is a marked decrease in drag when the spacing is reduced to half the lorry length, suggesting a more rapid reduction with a decrease in spacing when the spacing is small.

- Even at the largest spacing, there is a substantial reduction in the front face contribution to drag for the second vehicle. This suggests that wind tunnel studies should often consider the influence of the leading vehicle, as vehicles on busy motorways may travel at a comparable spacing even if not intentionally platooning.

- At the closest spacing, the mean drag coefficient across each lorry is 0.27 ± 0.03, giving a reduction of at least 48%, accounting for uncertainty, compared to lorries in isolation. Thus, the aerodynamic benefits of running lorries in a long platoon are substantial.

The slipstream and surface pressure measurements presented here will be valuable in validating numerical models, as data with platoons consisting of large numbers of vehicles are sparse. In addition to the mean flow analysis, the data collected will also be valuable in analysing unsteady effects such as the variation in the lateral force which will affect vehicle handling. These areas are recommended for further study.

Acknowledgements

References

[1] A. Iliaifar. Lidar, lasers, and logic: Anatomy of an autonomous vehicle. Available: https://www.digitaltrends.com/cars/lidar-lasers-and-beefed-up-computers-the-intricate-anatomy-of-an-autonomous-vehicle [accessed 4 July 2019], 2013.

[2] P. Goldin. 10 advantages of autonomous vehicles. Itsdigest. Available: http://www.itsdigest.com/10-advantages-autonomous-vehicles [accessed 4 July 2019], 2018.

[3] CORDIS. Periodic Report Summary 2 - SARTRE (Safe road trains for the environment; developing strategies and technologies to allow vehicle platoons to operate on normal public highways). Available: https://cordis.europa.eu/result/rcn/58617_en.html [accessed 4 July 2019], 2012.

[4] E. Chan. Overview of the SARTRE Platooning Project: Technology Leadership Brief. SAE Technical Paper 2012-01-9019, 2012. https://doi.org/10.4271/2012-01-9019.

[5] A. Davila, E. Aramburu, and A. Freixas. Making the best out of aerodynamics: Platoons. SAE Technical paper 2013-01-0767, 2013. https://doi.org/10.4271/2013-01-0767.

[6] S. Eilers, J. Mårtensson, H. Pettersson, M. Pillado, D. Gallegos, M. Tobar, K. H. Johansson, X. Ma, T. Friedrichs, S. S. Borojeni and M. Adolfson. COMPANION - Towards Co-Operative Platoon Management of Heavy-Duty Vehicles. *Proceedings of the IEEE 18th International Conference on Intelligent Transportation Systems*, 1267-1273, 2015. https://doi.org/10.1109/ITSC.2015.208.

[7] Department for Transport, Highways England, and Centre for Connected and Autonomous Vehicles. Green light for lorry 'platooning'. Available: https://www.gov.uk/government/news/green-light-for-lorry-platooning [accessed 4 July 2019], 2017.

[8] BBC News. 'Self-driving' lorries to be tested on UK roads. Available: https://www.bbc.co.uk/news/technology-41038220 [accessed 4 July 2019], 2017.

[9] S. Fallah. We're not ready for driverless cars. Available: https://www.weforum.org/agenda/2018/04/driverless-cars-are-forcing-cities-to-become-smart [accessed 4 July 2019], 2018.

[10] J. Manyika, M. Chui, J. Bughin, R. Dobbs, P. Bisson and A. Marrs. Disruptive technologies: Advances that will transform life, business, and the global economy. McKinsey Global Institute, 2013.

[11] J. Katz. Aerodynamics of race cars. *Annual Review of Fluid Mechanics*, 38(1):27–63, 2006. https://doi.org/10.1146/annurev.fluid.38.050304.092016.

[12] B. Blocken, T. van Druenen, Y. Toparlar, F. Malizia, P. Mannion, T. Andrianne, T. Marchal, G.- J. Maas and J. Diepens. Aerodynamic drag in cycling pelotons: New insights by CFD simulation and wind tunnel testing. *Journal of Wind Engineering and Industrial Aerodynamics*, 179:319-337, 2018. https://doi.org/10.1016/j.jweia.2018.06.011.

[13] H. Ebrahim. Analysis of the surface pressure and power consumption experienced by full-scale vehicles in platoon. *Proceedings of the Institution of Mechanical Engineers International Conference on Vehicle Aerodynamics*, 2018.

[14] R. Veldhuizen, G.M.R. Van Raemdonck and J.P. van der Krieke. Fuel economy improvement by means of two European tractor semi-trailer combinations in a platooning formation. *Journal of Wind Engineering & Industrial Aerodynamics,* 188:217–234, 2019. https://doi.org/10.1016/j.jweia.2019.03.002.

[15] M. Zabat, N. Stabile, S. Farascaroli, and F. Browand. The aerodynamic performance of platoons: A final report. *UC Berkeley: California Partners for Advanced Transportation Technology*, 1995.

[16] L. Tsuei and Ö. Savaş. Transient aerodynamics of vehicle platoons during in-line oscillations. *Journal of Wind Engineering and Industrial Aerodynamics*, 89(13):1085–1111, 2001. https://doi.org/10.1016/S0167-6105(01)00073-3.

[17] R. M. Pagliarella, S. Watkins, and A. Tempia. Aerodynamic performance of vehicles in platoons: The influence of backlight angles. SAE Technical Paper 2007-01-1547, 2007. https://doi.org/10.4271/2007-01-1547.

[18] S. Watkins and G. Vino. The effect of vehicle spacing on the aerodynamics of a representative car shape. *Journal of Wind Engineering and Industrial Aerodynamics*, 96(6):1232–1239, 2008. 5th International Colloquium on Bluff Body Aerodynamics and Applications. https://doi.org/10.1016/j.jweia.2007.06.042.

[19] G. Le Good, M. Resnick, P. Boardman, and B. Clough. Aerodynamic Design for Advanced Vehicle Platooning Concepts. *Proceedings of the third international conference in numerical and experimental aerodynamics of road vehicles and trains (Aerovehicles 3)*, 2018.

[20] G. Le Good, M. Resnick, P. Boardman, and B. Clough. Effects on the Aerodynamic Characteristics of Vehicles in Longitudinal Proximity Due to Changes in Style. SAE Technical Paper 2018-37-0018, 2018. https://doi.org/10.4271/2018-37-0018.

[21] P. Vegendla, T. Sofu, R. Saha, M. Madurai Kumar, and L.-K. Hwang. Investigation of aerodynamic influence on truck platooning. SAE Technical Paper 2015-01-2895, 2015. https://doi.org/10.4271/2015-01-2895.

[22] H. Humphreys and D. Bevly. Computational fluid dynamic analysis of a generic 2 truck platoon. SAE Technical Paper 2016-01-8008, 2016. https://doi.org/10.4271/2016-01-8008.

[23] M. Mirzaei and S. Krajnovic′. Large eddy simulations of flow around two generic vehicles in a platoon. In A. Segalini, editor, *Proceedings of the 5th International Conference on Jets, Wakes and Separated Flows (ICJWSF2015)*, 283–288, Springer International Publishing, 2016. https://doi.org/10.1007/978-3-319-30602-5_35.

[24] E. Jacuzzi and K. Granlund. Passive flow control for drag reduction in vehicle platoons. Journal of Wind Engineering & Industrial Aerodynamics 189:104–117, 2019. https://doi.org/10.1016/j.jweia.2019.03.001.

[25] B. Blocken, Y. Toparlar and T. Andrianne. Aerodynamic benefit for a cyclist by a following motorcycle. *Journal of Wind Engineering and Industrial Aerodynamics*, 155:1-10, 2016. https://doi.org/10.1016/j.jweia.2016.04.008.

[26] B. Blocken and Y. Toparlar. A following car influences cyclist drag: CFD simulations and wind tunnel measurements. *Journal of Wind Engineering and Industrial Aerodynamics*, 145:178-186, 2015. https://doi.org/10.1016/j.jweia.2015.06.015.

[27] C. J. Baker, S. J. Dalley, T Johnson, A Quinn, and N. G. Wright. The slipstream and wake of a high-speed train. *Proceedings of the Institution of Mechanical Engineers, Part F: Journal of Rail and Rapid Transit*, 215(2):83–99, 2001. https://doi.org/10.1243/0954409011531422.

[28] D. Soper, M. Gallagher, C. Baker, and A. Quinn. A model-scale study to assess the influence of ground geometries on aerodynamic flow development around a train. *Proceedings of the Institution of Mechanical Engineers, Part F: Journal of Rail and Rapid Transit*, 2016. https://doi.org/10.1177/0954409716648719.

[29] A. D. Quinn, M. Sterling, A. P. Robertson, and C. J. Baker. An investigation of the wind-induced rolling moment on a commercial vehicle in the atmospheric boundary layer. *Proceedings of the Institution of Mechanical Engineers, Part D: Journal of Automobile Engineering*, 221(11):1367–1379, 2007. https://doi.org/10.1243/09544070JAUTO537.

[30] M. Sterling, A. D. Quinn, D. M. Hargreaves, F. Cheli, E. Sabbioni, G. Tomasini, D. Delaunay, C. J. Baker and H. Morvan. A comparison of different methods to evaluate the wind induced forces on a high sided lorry. *Journal of Wind Engineering and Industrial Aerodynamics*, 98:10–20, 2010. https://doi.org/10.1016/j.jweia.2009.08.008.

[31] F. Cheli, R. Corradi, E. Sabbioni and G. Tomasini. Wind tunnel tests on heavy road vehicles: Cross wind induced loads — Part 1. *Journal of Wind Engineering and Industrial Aerodynamics*, 99(10): 1000–1010, 2011. https://doi.org/10.1016/j.jweia.2011.07.009.

[32] N. Patel, H. Hemida and A. Quinn. Large-Eddy Simulations of the airflow around a vehicle.

Proceedings of the 6th European and African Conference on Wind Engineering (EACWE2013), 2013.

[33] D. Soper, C. Baker, and M. Sterling. Experimental investigation of the slipstream development around a container freight train using a moving model facility. *Journal of Wind Engineering and Industrial Aerodynamics*, 135:105–117, 2014. https://doi.org/10.1016/j.jweia.2014.10.001.

[34] F. Dorigatti, M. Sterling, C. J. Baker, and A. D. Quinn. Crosswind effects on the stability of a model passenger train - a comparison of static and moving experiments. *Journal of Wind Engineering and Industrial Aerodynamics*, 138:36–51, 2015. https://doi.org/10.1016/j.jweia.2014.11.009.

[35] TFI. Turbulent Flow Instrumentation - Cobra Probe - Getting started guide. Technical report, Turbulent Flow Instrumentation, 2011.

[36] D. Soper, D. Flynn, C. Baker, A. Jackson, and H. Hemida. A comparative study of methods to simulate aerodynamic flow beneath a high-speed train. *Proceedings of the Institution of Mechanical Engineers, Part F: Journal of Rail and Rapid Transit*, 232(5):1464–1482, 2018. https://doi.org/10.1177/0954409717734090.

[37] FirstSensor. HCLA Series miniature amplified low pressure sensors - Data Sheet. 2018.

[38] D. Soper. The aerodynamics of a container freight train. Ph. D. thesis, University of Birmingham, 2014.

[39] J. R. Taylor. An introduction to error analysis: the study of uncertainties in physical measurements. University science books, New York, 1997.

[40] F. Dorigatti. Rail vehicles in crosswinds: analysis of steady and unsteady aerodynamic effects through static and moving model tests. Ph. D. thesis, University of Birmingham, 2013.

[41] F. Dionori, L. Casullo, S. Ellis, D. Ranghetti, K. Bablinski, C. Vollath and C. Soutra. Freight on road: why EU shippers prefer truck to train. Directorate-general for international policies. Policy department B. Structural and Cohesion policies. *Transport and Tourism*, 2015.

[42] Rail Accident Investigation Branch. Report 01/2017: Wheelchair contacting a train at Twyford station. Available: https://www.gov.uk/government/news/report-012017-wheelchair-contacting-a-train-at-twyford-station [accessed 4 July 2019], 2017.

[43] Railway Safety and Standards Board. Parents alerted to pushchair risk on platforms. Available: https://www.rssb.co.uk/News/Pages/parents-alerted-to-pushchair-risk-on-platforms.aspx

[accessed 4 July 2019], 2017.

[44] Maidenhead Advertiser. Rail inspectors investigating after pram is sucked into train path. Available: https://www.maidenhead-advertiser.co.uk/gallery/maidenhead/129978/rail-inspectors-investi gating-after-empty-pram-is-dragged-into-train-path.html [accessed 4 July 2019], 2018.

[45] R. P. Hoxey, P. J. Richards and J. L. Short. A 6 m cube in an atmospheric boundary layer flow Part 1. Full-scale and wind tunnel results. *Wind and Structures*, 5(2-4):165–176, 2002. https://doi.org/10.4271/2008-01-0658.

[46] J. W. Allan. Aerodynamic drag and pressure measurements on a simplified tractor-trailer model. *Journal of Wind Engineering and Industrial Aerodynamics*, 9:125-136, 1981. https://doi.org/10.1016/0167-6105(81)90083-0.

[47] R. Dominy and G. Le Good. The use of a Bluff Body Wake Generator for Wind Tunnel Studies of NASCAR Drafting Aerodynamics. *SAE International Journal of Passenger Cars - Mechanical Systems,* 1(1):1404-1410, 2009. https://doi.org/10.4271/2008-01-2990.

[48] M. Wilson, R. Dominy and A. Straker. The Aerodynamic Characteristics of a Race Car Wing Operating in a Wake. *SAE International Journal of Passenger Cars - Mechanical Systems,* 1(1):552-559, 2009. https://doi.org/10.4271/2008-01-0658.